



HAL
open science

The Variable Sampling Interval EWMA \bar{X} Chart with Estimated Process Parameters

Wei Lin Teoh, L. Ong, Michael Khoo, Philippe Castagliola, Z. Chong

► **To cite this version:**

Wei Lin Teoh, L. Ong, Michael Khoo, Philippe Castagliola, Z. Chong. The Variable Sampling Interval EWMA \bar{X} Chart with Estimated Process Parameters. *Journal of Testing and Evaluation*, 2019, 49 (2), pp.1237-1265. 10.1520/JTE20180058 . hal-03146344

HAL Id: hal-03146344

<https://hal.science/hal-03146344>

Submitted on 19 Aug 2021

HAL is a multi-disciplinary open access archive for the deposit and dissemination of scientific research documents, whether they are published or not. The documents may come from teaching and research institutions in France or abroad, or from public or private research centers.

L'archive ouverte pluridisciplinaire **HAL**, est destinée au dépôt et à la diffusion de documents scientifiques de niveau recherche, publiés ou non, émanant des établissements d'enseignement et de recherche français ou étrangers, des laboratoires publics ou privés.

The Variable Sampling Interval EWMA \bar{X} Chart with Estimated Process Parameters

W.L. Teoh (Corresponding author)

School of Mathematical and Computer Sciences,

Heriot-Watt University Malaysia,

62200 Putrajaya, Malaysia

weilin.teoh@gmail.com

Tel: +603-88943888; Fax: +603-88943999

L.V. Ong

Department of Physical and Mathematical Science, Faculty of Science,

Universiti Tunku Abdul Rahman, 31900 Kampar, Perak, Malaysia

elvyong88@hotmail.com

Michael B.C. Khoo

School of Mathematical Sciences,

Universiti Sains Malaysia, 11800 Penang, Malaysia

mkbc@usm.my

Philippe Castagliola

Université de Nantes & LS2N UMR 6004, Nantes, France

philippe.castagliola@univ-nantes.fr

Z.L. Chong

Department of Physical and Mathematical Science, Faculty of Science,

Universiti Tunku Abdul Rahman, 31900 Kampar, Perak, Malaysia

chongzl@utar.edu.my

The Variable Sampling Interval EWMA \bar{X} Chart with Estimated Process Parameters

ABSTRACT

The exponentially weighted moving average (EWMA) \bar{X} chart with the variable-sampling-interval (VSI) feature is usually scrutinized under the assumption of known process parameters. However, in practice, process parameters are usually unknown and they need to be estimated from the in-control Phase-I dataset. With this in mind, this paper proposes the VSI EWMA \bar{X} chart where the process parameters are estimated. A Markov Chain approach is adopted to derive the run-length properties of the VSI EWMA \bar{X} chart with estimated process parameters. The standard deviation of the average time to signal (SDATS) is employed to measure the practitioner-to-practitioner variation in the control chart's performance. This variation occurs because different Phase-I datasets are used among practitioners to estimate the process parameters. Based on the SDATS criterion, this paper provides recommendations regarding the minimum number of required Phase-I samples. For an optimum implementation, this paper develops two optimization algorithms for the VSI EWMA \bar{X} chart with estimated process parameters, i.e. by minimizing the (i) out-of-control AATS (expected value of the average time to signal) and (ii) out-of-control EAATS (expected value of the AATS), for the cases of deterministic and unknown shift sizes, respectively. With the implementation of these new design procedures, the VSI EWMA \bar{X} chart with estimated process parameters is not only able to achieve a desirable in-control performance, but it is also able to quickly detect changes in the process.

Keywords: expected value of the average time to signal, known and unknown shift sizes, optimization design, parameter estimation, standard deviation of the average time to signal, standard deviation of the time to signal

1. Introduction

Contemporarily, controlling and improving quality are vitally viewed in the global market. A business that can delight customers with improved quality of products and services, dominates and establishes good reputation in the business world. A control chart is an excellent process monitoring technique to reduce variability in key parameters. A well-designed control chart enables practitioners to quickly detect process shifts before manufacturing many nonconforming products. Some recent studies regarding control charts are those by Chong et al. [1], Kang et al. [2], Teoh et al. [3, 4] and Yeong et al. [5]. There are two phases of process

monitoring in the application of control charts. In Phase-I, an in-control dataset is collected and analyzed in a retrospective analysis. Then, appropriate control limits are computed in Phase-I in order to monitor Phase-II production. In Phase-II, a control chart is prospectively used to detect changes that occur at an unknown time point.

The vast majority of researches on process monitoring focuses on the formulation of Phase-II control charts. Particular attention has been devoted to the development of adaptive control schemes as they are more sensitive for the detection of small to moderate shifts compared to the fixed control schemes. Adaptive charts allow the charts' parameters, i.e. the sample size, sampling interval, and / or control limits' coefficient, to vary depending on the location of the previous sample statistic plotted on the chart. A control chart with the feature of variable sampling intervals (VSI) is one of the adaptive charts. In a VSI chart, the next sampling interval is long, when there is no indication of process changes; while the next sampling interval is short, whenever there is an indication that an out-of-control situation is likely to occur. To enhance the inspection efficiency of the fixed-sampling-interval (FSI) Exponentially Weighted Moving Average (EWMA) \bar{X} chart, Saccucci, Amin, and Lucas [6] adopted the VSI feature in designing the EWMA \bar{X} chart. The VSI R -EWMA and VSI S^2 -EWMA charts proposed by Castagliola et al. [7, 8], respectively, substantially enhance the statistical efficiency of their corresponding FSI charts. The VSI EWMA chart shows a significant improvements in detecting process mean shifts under both cases of normality and non-normality (Lin and Chou [9]). Economic models of the VSI EWMA charts were developed by Chou, Chen, and Liu [10] and Xue, Xu, and Liu [11] under the cases of normality and non-normality, respectively. Their proposed economic models are able to reduce the expected total cost and process production cycle cost. Yang [12] demonstrated that the VSI EWMA average loss chart is effective in monitoring the process mean and variability simultaneously. This leads to a reduction of the required time, resources and efforts in implementing the control charting method. The VSI EWMA chart for monitoring the coefficient of variation remarkably outperforms its corresponding Shewhart, VSI, Synthetic and FSI EWMA charts (Yeong et al. [13]). Due to the attractiveness of the VSI EWMA chart, Yang and Yu [14, 15] applied the VSI EWMA charts to monitor the process mean of a cascade process and an automobile braking system with incorrect adjustment, respectively.

As in the case of most control charts, the VSI EWMA charts are typically designed with the assumption that the quality characteristic is normally distributed with known process mean and variance. The fact that traditional control charts require full knowledge of the process

parameters in Phase-I, is not practical in real life and industrial applications. These process parameters are usually unknown and they need to be estimated from an in-control Phase-I dataset. Jensen et al. [16] and Psarakis, Vyniou, and Castagliola [17] provided a comprehensive literature review on the performance of control charts when the process parameters are estimated. It has been long recognized that by using estimates in place of known process parameters, the performance of the control chart is significantly degraded (see, for example, Epprecht, Loureiro, and Chakraborti [18]; Jones, Champ, and Rigdon [19]; Quinino, Ho, and Trindade [20]). This is due to the additional variability of the estimates computed from the Phase-I process. Jones [21] stated that the EWMA chart that fails to account for process-parameter estimates, has an increase in the false alarm rate and a reduction in the detection ability of process changes. To address these problems, much efforts have been devoted to design control charts by accurately accounting for process-parameter estimates (see, for example, Hany and Mahmoud [22]; Lim et al. [23]; Saleh et al. [24]; Teoh et al. [25]; Zhang et al. [26]). Since control charts with the VSI feature are more sensitive to small shifts, Jensen et al. [16] noted that these type of control charts are more seriously influenced by process parameter estimation. Therefore, the issue of unknown process parameters of the VSI EWMA \bar{X} chart remains a practical problem to practitioners. This setback motivates the design of an optimal VSI EWMA \bar{X} chart with estimated process parameters in this paper.

In this paper, we investigate the performance of the VSI EWMA \bar{X} chart when process parameters are estimated. To the best of the authors' knowledge, this issue has not been addressed in the existing literature. The performance of Phase-II control charts are commonly evaluated using the average time to signal (ATS) and standard deviation of the time to signal (SDTS) criteria. Note that both ATS and SDTS become random variables when process parameters are estimated as different Phase-I data sets are being adopted by practitioners. This leads to randomness in the chart's performance among practitioners, namely practitioner-to-practitioner variation. Therefore, for complete evaluation, the VSI EWMA \bar{X} chart with estimated process parameters is evaluated, in terms of the expected value of the ATS (AATS), average of the SDTS (ASDTS) and standard deviation of the ATS (SDATS). Unlike ATS and SDTS, AATS and ASDTS are obtained by averaging all possible values of the parameter estimates. Note that the SDATS is analyzed in this paper to account for practitioner-to-practitioner variability in the control chart's performance. A similar performance metric, i.e. the standard deviation of the average run length (SDARL) was proposed by Jones and Steiner [27] and further used by Faraz, Woodall, and Heuchenne [28], Saleh et al. [24], and Zhang,

Megahed, and Woodall [29]. Moreover, by means of the Markov chain approach, the AATS, ASDTS, SDATS, expected value of the average sampling interval (AASI) and expected value of the AATS (EAATS), specifically for the VSI EWMA \bar{X} chart with estimated process parameters, are derived in this paper. Both zero and steady states are considered. The zero-state run lengths are the run lengths of a control chart initialized at the initial state; while the steady-state run lengths are the run lengths of a control chart observed after the control statistic has reached the steady state. Using these formulae, the characteristics of the run-length and optimal chart's parameters of the VSI EWMA \bar{X} chart with estimated process parameters can easily be obtained.

In practice, it is important for quality practitioners to compute the optimal parameters of the VSI EWMA \bar{X} chart with estimated process parameters, in order to optimally implement the proposed chart. In this paper, we optimally design the VSI EWMA \bar{X} chart with estimated process parameters by minimizing the (i) out-of-control AATS ($AATS_1$) and (ii) out-of-control EAATS ($EAATS_1$), for the cases of deterministic and unknown shift sizes, respectively. The unknown shift-size condition is vitally viewed recently. In reality, the size of a process shift in the future is usually unknown. This will lead to a poor performance if the actual shift size is not the same as the one adopted in the design of the VSI EWMA \bar{X} chart with estimated process parameters. To cope with this random shift-size problem, the EAATS which is the AATS integrated over a shift-size distribution, is proposed in this paper. A similar approach was suggested by Castagliola, Celano, and Psarakis [30], Celano et al. [31], and Wu, Shamsuzzaman, and Pan [32], in designing control charts with known process parameters.

The remainder of this paper is structured as follows: In Section 2, we review the operation of the VSI EWMA \bar{X} chart. The run-length properties of the VSI EWMA \bar{X} chart with known and estimated process parameters are presented in Section 3. Section 4 compares the VSI EWMA \bar{X} chart's performance between the cases of known and estimated process parameters. Section 5 suggests two optimal-design procedures for the VSI EWMA \bar{X} chart with estimated process parameters, i.e. by minimizing the (i) $AATS_1$ and (ii) $EAATS_1$. A comparison between the zero-state and steady-state performances of the VSI EWMA \bar{X} chart with known and estimated process parameters are discussed in Section 6. The VSI EWMA \bar{X} chart with estimated process parameters is implemented with real data in Section 7. Finally, conclusions are drawn in Section 8.

2. The VSI EWMA \bar{X} chart

Assume that $(Y_{i,1}, Y_{i,2}, \dots, Y_{i,n})$ is a Phase-II sample of n independent and identically distributed normal random variables, i.e. $Y_{ij} \sim N(\mu, \sigma_0^2)$ for $i = 1, 2, \dots$ and $j = 1, 2, \dots, n$. Here, μ and σ_0^2 are the mean and in-control variance, respectively. When the process parameters are known, the VSI EWMA \bar{X} chart's statistic at time i is defined as

$$Z_i = \lambda W_i + (1 - \lambda)Z_{i-1}, \text{ for } i = 1, 2, \dots, \quad (1)$$

where the initial value $Z_0 = \mu_0$. In Equation (1), λ is a smoothing constant such that $0 < \lambda \leq 1$ and W_i is the standardized sample mean when the process is in-control, i.e.

$$W_i = \frac{\bar{Y}_i - \mu_0}{\sigma_0/\sqrt{n}}, \quad (2)$$

where \bar{Y}_i is the sample mean of the i^{th} sample and μ_0 is the in-control mean.

Because of standardization, the upper control limit (UCL) and lower control limit (LCL) of the VSI EWMA \bar{X} chart are

$$\text{UCL/LCL} = \pm K_2 \sqrt{\frac{\lambda}{2 - \lambda}}, \quad (3)$$

where K_2 is the control limit coefficient of the VSI EWMA \bar{X} chart. The upper warning limit (UWL) and lower warning limit (LWL) of the VSI EWMA \bar{X} chart can be written as

$$\text{UWL/LWL} = \pm K_1 \sqrt{\frac{\lambda}{2 - \lambda}}, \quad (4)$$

where K_1 is the warning limit coefficient. Note that $K_1 > 0$ and $K_2 > K_1$.

A graphical view of the VSI EWMA \bar{X} chart is shown in Figure 1. The VSI EWMA \bar{X} chart divides the chart into three regions, which are the safe region, the warning region, and the out-of-control region. In this paper, we assume that the VSI EWMA \bar{X} chart only takes two sampling intervals, i.e. the long (h_1) and short (h_2) sampling intervals, such that $h_1 > h_2$. Reynolds et al. [33] showed that the detection effectiveness of the VSI scheme can be achieved by using only two sampling intervals; thus the complexity of the chart can be maintained in a favorable situation. The operation of the VSI EWMA \bar{X} chart is described as follows:

Step 1: Take a sample of n observations.

Step 2: Compute the standardized sample mean (W_i) and control charting statistic (Z_i) as in Equations (2) and (1), respectively.

Step 3: If the control statistic falls in the safe region, i.e. $Z_i \in [\text{LWL}, \text{UWL}]$, the process is declared as in-control and the next sample is taken after a long sampling interval (h_1).

Step 4: If the control statistic falls in the warning region, i.e. $Z_i \in [\text{LCL}, \text{LWL}) \cup (\text{UWL}, \text{UCL}]$, the process is still considered as in-control and the next sample is taken after a short sampling interval (h_2) in order to tighten the process.

Step 5: If the control statistic falls in the out-of-control region, i.e. $Z_i > \text{UCL}$ or $Z_i < \text{LCL}$, the process is declared as out-of-control. Assignable cause(s) must be searched and discarded.

3. The run-length properties of the VSI EWMA \bar{X} chart

3.1 The VSI EWMA \bar{X} chart with known process parameters

The Markov chain approach, originally proposed by Brook and Evans [34], is adopted to evaluate the run-length properties of the VSI EWMA \bar{X} chart. Specifically, by referring to Figure 2, the interval between UCL and LCL is divided into $2g + 1$ subintervals, each of width $2d$, where $2d = (\text{UCL} - \text{LCL}) / (2g + 1)$. A sufficiently large number of subintervals (say $g = 100$, i.e. $2g + 1 = 201$) will enhance this finite approach to accurately evaluate the run-length properties of the VSI EWMA \bar{X} chart. If $H_\gamma - d < Z_i < H_\gamma + d$, for $\gamma = -g, \dots, -1, 0, 1, \dots, g$, the control charting statistic (Z_i) is in the transient state γ at time i ; otherwise, Z_i is in the absorbing state, i.e. $Z_i \in (-\infty, \text{LCL}) \cup (\text{UCL}, +\infty)$. Here, H_γ is the midpoint of the γ^{th} subinterval. Let \mathbf{R} be the $(2g + 1) \times (2g + 1)$ matrix of probabilities ($R_{k,\gamma}$) for the $(2g + 1)$ transient states, i.e.

$$\mathbf{R} = \begin{pmatrix} R_{-g,-g} & \cdots & R_{-g,-1} & R_{-g,0} & R_{-g,+1} & \cdots & R_{-g,+g} \\ \vdots & \vdots & \vdots & \vdots & \vdots & \vdots & \vdots \\ R_{-1,-g} & \cdots & R_{-1,-1} & R_{-1,0} & R_{-1,+1} & \cdots & R_{-1,+g} \\ R_{0,-g} & \cdots & R_{0,-1} & R_{0,0} & R_{0,+1} & \cdots & R_{0,+g} \\ R_{+1,-g} & \cdots & R_{+1,-1} & R_{+1,0} & R_{+1,+1} & \cdots & R_{+1,+g} \\ \vdots & \vdots & \vdots & \vdots & \vdots & \vdots & \vdots \\ R_{+g,-g} & \cdots & R_{+g,-1} & R_{+g,0} & R_{+g,+1} & \cdots & R_{+g,+g} \end{pmatrix}. \quad (5)$$

Then, the transition probabilities ($R_{k,\gamma}$), for $k, \gamma = -g, \dots, -1, 0, 1, \dots, g$, are equal to

$$R_{k,\gamma} = \Phi\left(\frac{H_\gamma + d - (1-\lambda)H_k}{\lambda} - \delta\sqrt{n}\right) - \Phi\left(\frac{H_\gamma - d - (1-\lambda)H_k}{\lambda} - \delta\sqrt{n}\right), \quad (6)$$

where $\Phi(\cdot)$ represents the standard normal cumulative distribution function (cdf) and δ is the magnitude of the standardized mean shift, i.e. $\delta = |\mu_1 - \mu_0| / \sigma_0$. Here, μ_1 is the out-of-control mean. If $\delta = 0$, the process is in-control; otherwise, it is out-of-control.

By using the Markov chain approach, the conditional zero-state ATS and SDTS of the VSI EWMA \bar{X} chart are computed as (Saccucci, Amin and Lucas [6])

$$\text{ATS} = \mathbf{q}^T \mathbf{Q} \mathbf{b} - \mathbf{q}^T \mathbf{b} = \mathbf{q}^T (\mathbf{Q} - \mathbf{I}) \mathbf{b}, \quad (7)$$

and

$$\text{SDTS} = \sqrt{\mathbf{q}^T \mathbf{Q} \mathbf{B} (\mathbf{2Q} - \mathbf{I}) \mathbf{b} - (\mathbf{q}^T \mathbf{Q} \mathbf{b})^2}, \quad (8)$$

respectively, where $\mathbf{q} = (0, \dots, 1, \dots, 0)^T$ is the $(2g + 1) \times 1$ initial probability vector with all the elements equal to zero except the state $g + 1$ which is unity. Note that unity in state $g + 1$ corresponds to the state containing μ_0 . Also, in Equations (7) and (8), $\mathbf{Q} = (\mathbf{I} - \mathbf{R})^{-1}$ is the fundamental matrix, \mathbf{I} is an identity matrix, \mathbf{b} is the vector of sampling intervals (with entries h_1 or h_2) corresponding to the discretized states of the Markov chain, and \mathbf{B} is a diagonal matrix with the γ^{th} element equal to b_γ . Here, b_γ represents the sampling interval when Z_i is in state H_γ , i.e.

$$b_\gamma = \begin{cases} h_1, & \text{LWL} < H_\gamma < \text{UWL} \\ h_2, & \text{otherwise} \end{cases}. \quad (9)$$

For the steady-state case, we adopt the cyclical steady-state vector of probabilities (\mathbf{q}_{ss}) proposed by Darroch and Seneta [35], i.e.

$$\mathbf{q}_{ss} = \frac{(\mathbf{I} - \mathbf{R}^T)^{-1} \mathbf{q}}{\mathbf{1}^T (\mathbf{I} - \mathbf{R}^T)^{-1} \mathbf{q}}. \quad (10)$$

The cyclical steady-state probability vector (\mathbf{q}_{ss}) is computed assuming that the Markov chain restarts with the initial probability vector \mathbf{q} when it reaches the absorbing state. Therefore, the conditional steady-state ATS and SDTS of the VSI EWMA \bar{X} chart can easily be obtained by replacing \mathbf{q} in Equations (7) and (8) with \mathbf{q}_{ss} . Then the conditional steady-state ATS and SDTS become

$$\text{ATS} = \mathbf{q}_{ss}^T \mathbf{Q} \mathbf{b} - \mathbf{q}_{ss}^T \mathbf{b} = \mathbf{q}_{ss}^T (\mathbf{Q} - \mathbf{I}) \mathbf{b}, \quad (11)$$

and

$$\text{SDTS} = \sqrt{\mathbf{q}_{ss}^T \mathbf{Q} \mathbf{B} (\mathbf{2Q} - \mathbf{I}) \mathbf{b} - (\mathbf{q}_{ss}^T \mathbf{Q} \mathbf{b})^2}, \quad (12)$$

respectively.

To have a fair comparison with other FSI control charts, it is important that the in-control ASI (ASI_0) of the VSI EWMA \bar{X} chart is equal to the sampling interval of the FSI charts. To the best of the authors' knowledge, all the existing literatures do not disclose how the ASI formula is actually derived. In this paper, we propose a simple formula to solve this problem. Note that the ASI of the VSI EWMA \bar{X} chart corresponds to a process functioning over an infinite horizon. Therefore, \mathbf{q}_{ss} is applied in our ASI formula. Since the probabilities of the

vector \mathbf{q}_{ss} are associated with the long (h_1) and short (h_2) sampling intervals of vector \mathbf{b} , the conditional ASI can easily be computed by

$$\text{ASI} = \mathbf{1}^T (\mathbf{q}_{ss} \odot \mathbf{b}), \quad (13)$$

where $\mathbf{1} = (1, 1, \dots, 1)^T$ and \odot is the element-wise multiplication of the vectors.

3.2 The VSI EWMA \bar{X} chart with estimated process parameters

When μ_0 and σ_0 are unknown, they have to be estimated from m in-control Phase-I samples, each containing n measurements $\{X_{i,1}, X_{i,2}, \dots, X_{i,n}\}$, for $i = 1, 2, \dots, m$. The measurements within and between samples are assumed to be independent and $X_{i,j} \sim N(\mu, \sigma_0^2)$. The commonly used estimator $\hat{\mu}_0$ of parameter μ_0 is the grand mean, i.e.

$$\hat{\mu}_0 = \frac{1}{m} \sum_{i=1}^m \bar{X}_i, \quad (14)$$

where $\bar{X}_i = \sum_{j=1}^n X_{i,j}/n$ is the sample mean of i^{th} sample. The unbiased estimator $\hat{\sigma}_0$ of parameter σ_0 is the pooled estimator (Jones [21]), i.e.

$$\hat{\sigma}_0 = \frac{S_{\text{pooled}}}{c_{4,m}}, \quad (15)$$

where $S_{\text{pooled}} = \sqrt{\sum_{i=1}^m \sum_{j=1}^n (X_{i,j} - \bar{X}_i)^2 / [m(n-1)]}$ and

$c_{4,m} = \left\{ \sqrt{2} \Gamma \left[\frac{(m(n-1)+1)}{2} \right] \right\} / \left\{ \sqrt{m(n-1)} \Gamma \left[\frac{(m(n-1))}{2} \right] \right\}$. Among all the five estimators of standard deviation considered in Saleh et al. [24], they showed that the estimator $\hat{\sigma}_0$ in Equation (15) is one of the best estimators. Therefore, Equation (15) is adopted in this paper to estimate the parameter σ_0 .

To compute the chart statistic Z_i of the VSI EWMA \bar{X} chart with estimated process parameters in Equation (1), replace W_i in Equation (2) with \hat{W}_i as follows:

$$\hat{W}_i = \frac{\bar{Y}_i - \hat{\mu}_0}{\hat{\sigma}_0 / \sqrt{n}}. \quad (16)$$

Then, the transition probability ($\hat{R}_{k,\gamma}$) for the transient states of the matrix $\hat{\mathbf{R}}$ is equal to

$$\begin{aligned} \hat{R}_{k,\gamma} = & \Phi \left[V \left(\frac{H_\gamma + d - (1-\lambda)H_k}{\lambda} \right) + \frac{U}{\sqrt{m}} - \delta\sqrt{n} \right] - \\ & \Phi \left[V \left(\frac{H_\gamma - d - (1-\lambda)H_k}{\lambda} \right) + \frac{U}{\sqrt{m}} - \delta\sqrt{n} \right]. \end{aligned} \quad (17)$$

The detailed derivation of $\hat{R}_{k,\gamma}$ in Equation (17) is shown in the Appendix. Note that matrix $\hat{\mathbf{R}}$ is matrix \mathbf{R} in Equation (5), for which the probabilities $R_{k,\gamma}$ are replaced by $\hat{R}_{k,\gamma}$. In Equation (17), the random variable V is defined as the ratio of the estimated in-control standard deviation to the actual in-control standard deviation of the process, i.e.

$$V = \frac{\hat{\sigma}_0}{\sigma_0}; \quad (18)$$

while the random variable U is the standardized distance from the estimated in-control process mean to the actual in-control process mean, i.e.

$$U = \frac{\hat{\mu}_0 - \mu_0}{\sigma_0 / \sqrt{mn}}. \quad (19)$$

It is known that V^2 follows a gamma distribution with parameters $[m(n-1)]/2$ and $2/[m(n-1)c_{4,m}^2]$, i.e. $V^2 \sim G([m(n-1)]/2, 2/[m(n-1)c_{4,m}^2])$ (Zhang et al. [26]). Therefore, the probability density function (pdf) of V is

$$f_V(v) = 2vf_G\left(v^2 \left| \frac{m(n-1)}{2}, \frac{2}{m(n-1)c_{4,m}^2} \right.\right), \quad (20)$$

where $f_G(\cdot)$ is the pdf of the gamma distribution with parameters $[m(n-1)]/2$ and $2/[m(n-1)c_{4,m}^2]$. The standard normal random variable U in Equation (19) follows the $N(0, 1)$ distribution. Hence, the pdf of U is

$$f_U(u) = \phi(u), \quad (21)$$

where $\phi(\cdot)$ denotes the pdf of a standard normal distribution.

By using the same Markov chain approach as for the case of known process parameters, the zero-state ATS of the VSI EWMA \bar{X} chart with estimated process parameters can be obtained as

$$\text{ATS} = \mathbf{q}^T \hat{\mathbf{Q}} \mathbf{b} - \mathbf{q}^T \mathbf{b} = \mathbf{q}^T (\hat{\mathbf{Q}} - \mathbf{I}) \mathbf{b}, \quad (22)$$

where $\hat{\mathbf{Q}} = (\mathbf{I} - \hat{\mathbf{R}})^{-1}$ is the fundamental matrix. Similarly, the steady-state ATS of the VSI EWMA \bar{X} chart with estimated process parameters can easily be obtained by replacing \mathbf{q} in Equation (22) with $\hat{\mathbf{q}}_{ss}$, where $\hat{\mathbf{q}}_{ss}$ is \mathbf{q}_{ss} in Equation (10), for which the matrix \mathbf{R} is replaced by $\hat{\mathbf{R}}$. Then the steady-state ATS becomes

$$\text{ATS} = \hat{\mathbf{q}}_{ss}^T \hat{\mathbf{Q}} \mathbf{b} - \hat{\mathbf{q}}_{ss}^T \mathbf{b} = \hat{\mathbf{q}}_{ss}^T (\hat{\mathbf{Q}} - \mathbf{I}) \mathbf{b}. \quad (23)$$

The zero- and steady-state ATSs in Equations (22) and (23), respectively, are functions of the random variables $\hat{\mu}_0$ and $\hat{\sigma}_0$, or similarly, the random variables U and V . Then, the unconditional zero- or steady-state AATS, which averages across the practitioner-to-practitioner variability, can be obtained as

$$\text{AATS} = E(\text{ATS}) = \int_{-\infty}^{\infty} \int_0^{\infty} \text{ATS} f_U(u) f_V(v) dvdu; \quad (24)$$

while the zero- or steady-state SDATS is obtained as

$$\text{SDATS} = \sqrt{E(\text{ATS}^2) - \text{AATS}^2}, \quad (25)$$

where $E(\text{ATS}^2) = \int_{-\infty}^{\infty} \int_0^{\infty} \text{ATS}^2 f_U(u) f_V(v) dvdu$. Note that for computing the zero-state AATS and SDATS, the zero-state ATS in Equation (22) is used; while for computing the steady-state AATS and SDATS, the steady-state ATS in Equation (23) is employed.

The unconditional zero-state ASDTS, which averages over all the possible values of the parameter estimations, is equal to

$$\text{ASDTS} = \sqrt{\int_{-\infty}^{\infty} \int_0^{\infty} \mathbf{q}^T \hat{\mathbf{Q}} \mathbf{B} (\mathbf{2}\hat{\mathbf{Q}} - \mathbf{I}) \mathbf{b} f_U(u) f_V(v) dvdu - \left[\int_{-\infty}^{\infty} \int_0^{\infty} \mathbf{q}^T \hat{\mathbf{Q}} \mathbf{b} f_U(u) f_V(v) dvdu \right]^2}. \quad (26)$$

By using a similar approach, the unconditional steady-state ASDTS is obtained by replacing \mathbf{q} in Equation (26) with $\hat{\mathbf{q}}_{ss}$, i.e.

$$\text{ASDTS} = \sqrt{\int_{-\infty}^{\infty} \int_0^{\infty} \hat{\mathbf{q}}_{ss}^T \hat{\mathbf{Q}} \mathbf{B} (\mathbf{2}\hat{\mathbf{Q}} - \mathbf{I}) \mathbf{b} f_U(u) f_V(v) dvdu - \left[\int_{-\infty}^{\infty} \int_0^{\infty} \hat{\mathbf{q}}_{ss}^T \hat{\mathbf{Q}} \mathbf{b} f_U(u) f_V(v) dvdu \right]^2}. \quad (27)$$

The difference between SDATS and ASDTS is that SDATS shows that the ATS is a random variable, which is not shown by ASDTS. Similarly, the unconditional AASI of the VSI EWMA \bar{X} chart with estimated parameters can be computed as

$$\text{AASI} = E(\text{ASI}) = \int_{-\infty}^{\infty} \int_0^{\infty} \mathbf{1}^T (\hat{\mathbf{q}}_{ss} \odot \mathbf{b}) f_U(u) f_V(v) dvdu. \quad (28)$$

The Gaussian quadrature method is employed to approximate the integrations in Equations (24) to (28); while the Monte Carlo simulation is used to validate the accuracy of all the numerical results presented in this paper.

4. A comparison of performances between the VSI EWMA \bar{X} chart with estimated and known process parameters

It is crucial to take note that the goal of this paper is to investigate the impact of Phase-I parameter estimation on the VSI EWMA \bar{X} chart's performance, instead of showing the superiority of the VSI EWMA \bar{X} chart over other control charts. For the VSI EWMA \bar{X} chart with estimated process parameters, the AATS, ASDTS and SDATS are used to evaluate the chart's performance. These performance measures are denoted as AATS₀, ASDTS₀ and SDATS₀ when the process is in-control; while AATS₁, ASDTS₁, and SDATS₁ are used to denote these measures for the out-of-control situation. On the contrary, the performance of the VSI EWMA \bar{X} chart with known process parameters, is evaluated using the ATS and SDTS criteria. When the process parameters are known, the ATS is a constant value; thus, the SDATS value is equal to zero. Similarly, the ATS₀ and SDTS₀ represent the in-control ATS and SDTS, respectively, for the VSI EWMA \bar{X} chart with known process parameters; while the ATS₁ and SDTS₁ represent the out-of-control ATS and SDTS, respectively.

Table 1 presents the zero-state AATS, ASDTS and SDATS values for the in-control and out-of-control cases of the VSI EWMA \bar{X} chart with estimated ($m \in \{25, 50, 100, 1000, 2000\}$) and known ($m = +\infty$) process parameters. Table 1 considers different combinations of chart's parameters (λ, K_1, K_2), sample size $n = 5$, ASI₀ = 1, standardized mean shifts $\delta \in \{0.2, 0.4, 0.6, 0.8, 1.0, 1.5, 2.0\}$, and sampling intervals $(h_1, h_2) \in \{(1.5, 0.5), (1.3, 0.1), (1.9, 0.1)\}$. The chart's parameters (λ, K_1, K_2) displayed in the second column of Table 1 are obtained by minimizing the zero-state ATS₁ of the VSI EWMA \bar{X} chart with known process parameters ($m = +\infty$), subject to the fixed values of zero-state ATS₀ = 370.40 and ASI₀ = 1. The results in columns 3 to 8 are computed using the specific combination of (λ, K_1, K_2) displayed in the second column of Table 1 and the formulae in Section 3. The values of the performance measures shown in the first row of each cell represent the in-control cases; while those shown in the second row of each cell represent the out-of-control cases. For example, when $\delta = 0.8$ and $(h_1, h_2) = (1.5, 0.5)$, the optimal chart's parameters (λ, K_1, K_2) for minimizing the zero-state ATS₁ are (0.346, 0.657, 2.946), for the VSI EWMA \bar{X} chart with known process parameters ($m = +\infty$). This set of parameters yields zero-state (ATS₀, SDTS₀) and (ATS₁, SDTS₁) values of (370.40, 369.94) and (1.72, 1.23), respectively, when $m = +\infty$. Also, when $m = 50$, the same set of chart's parameters (λ, K_1, K_2) = (0.346, 0.657, 2.946) gives zero-state (AATS₀, ASDTS₀, SDATS₀) = (323.37, 422.60, 192.98) and (AATS₁, ASDTS₁, SDATS₁) = (1.77, 1.36, 0.39) (see Table 1).

It is noticed in Table 1 that the results for the cases of estimated process parameters, are significantly different from that of the case with known process parameters, especially when

m and δ are small. This difference is due to the existence of variability in the process parameter estimation. For a fixed value of δ , the difference between the zero-state values of (AATS, ASDTS, SDATS) and (ATS, SDTS, SDATS) associated with estimated and known process parameters, respectively, generally reduces as m increases. Note that SDATS = 0 for all the cases of known process parameters. For instance, if $\delta = 0.2$ and $(h_1, h_2) = (1.9, 0.1)$, the zero-state $(AATS_1, ASDTS_1, SDATS_1) = (41.16, 114.93, 76.67)$ and $(20.80, 26.36, 13.69)$ for $m = 25$ and 100 , respectively, as opposed to the zero-state $(ATS_1, SDTS_1, SDATS_1) = (17.25, 14.56, 0)$ for $m = +\infty$ (see Table 1). The difference between the zero-state values of $(AATS_1, ASDTS_1, SDATS_1)$ and $(ATS_1, SDTS_1, SDATS_1)$ for the cases of estimated and known process parameters, respectively, becomes negligible even for small m when the mean shifts become large ($\delta \geq 1.5$). For small shifts ($\delta \leq 0.6$), it is observed from Table 1 that at least 1000 samples are needed for the chart with estimated process parameters to achieve a similar performance to the chart with known process parameters. For both the in-control and out-of-control cases, Table 1 clearly shows that as the zero-state SDATS decreases, the zero-state values of (AATS, ASDTS) converge to the corresponding zero-state values of (ATS, SDTS). Note that a small SDATS value indicates that the AATS value is close to the ATS value.

This paper also identifies the number of Phase-I samples m required to achieve a stable zero-state AATS performance and a sufficiently small value of SDATS. Zhang et al. [29] recommended that the SDATS value should be within 10% of the ATS value so that a reasonable chart performance can be attained, though it is still reflecting a considerable amount of variation. Table 2 gives the minimum number of Phase-I samples m required by the VSI EWMA \bar{X} chart with estimated process parameters, for both the in-control (first row of each cell) and out-of-control (second row of each cell) cases. This minimum number of m is obtained such that the zero-state SDATS value does not exceed 10% of the corresponding zero-state ATS value. In Table 2, we consider $\delta \in \{0.2, 0.4, 0.6, 0.8, 1.0, 1.5, 2.0\}$, $n = 5$ and $(h_1, h_2) \in \{(1.5, 0.5), (1.7, 0.3), (1.3, 0.1), (1.5, 0.1), (1.9, 0.1), (4.0, 0.1)\}$. It is a common practice to fix (h_1, h_2) . Therefore, the choice of the combinations of (h_1, h_2) throughout this paper is based on the recommendation by Reynolds et al. [33]. The optimal chart's parameters (λ, K_1, K_2) of the VSI EWMA \bar{X} chart with known process parameters ($m = +\infty$), which are listed in the last column of Tables 3 and 4, are adopted here to identify the minimum number of m required for all the cases considered in Table 2.

From Table 2, it is obvious that a large number of m , i.e. around 1000 to 1500 Phase-I samples are needed to attain a zero-state SDATS₀ that is within 10% of the desired zero-state

$ATS_0 = 370.40$. The minimum number of m (i.e. $m = 1400$ to 2000) required is more pronounced for a very small shift ($\delta = 0.2$). As expected, the minimum number of m required decreases as δ increases. For example, when $(h_1, h_2) = (1.5, 0.1)$, the VSI EWMA \bar{X} chart with estimated process parameters requires $m = 630$ when $\delta = 0.4$, but this value of m reduces to 90 when $\delta = 1.5$.

From Tables 1 and 2, it is obvious that a significant large number of Phase-I samples m is needed to achieve a reasonable control chart's performance. Nevertheless, using a large number of m is impractical in most applications. Also, from Tables 1 and 2, the zero-state $AATS_0$ values obtained for the cases of $\delta \leq 1.0$ or in other words, small λ , are generally lower than the desired zero-state ATS_0 , even for a very large m . This will lead to an unfavorable high false alarm rate. For example, when $(h_1, h_2) = (1.5, 0.5)$ and $\delta = 0.2$ (or $\lambda = 0.048$), the zero-state $AATS_0 = 350.37$ (see Table 2) of the estimated-parameter case, is lower than the zero-state $ATS_0 = 370.40$ of the corresponding known-parameter case. To overcome these problems, approaches based on bootstrapping the Phase-I data for the construction of an approximate confidence interval for the control limits was suggested by Gandy and Kvaløy [36]. Alternatively, since a very large number of m is unavailable at the initial state, Epprecht, Loureiro, and Chakraborti [18] suggested an alternative method that consists to start monitoring the arriving Phase-II samples by computing the trial control limits with the available Phase-I samples. Then, the trial control limits are kept revising periodically with the in-control data, until the required minimum number of in-control samples is obtained.

From Tables 1 and 2, we can conclude that the optimal chart's parameters for the case of known process parameters are inappropriate to be used in the case of estimated process parameters. Therefore, new optimal chart's parameters (λ, K_1, K_2) specially designed for the VSI EWMA \bar{X} chart with estimated process parameters need to be proposed in this paper (see Section 5). As pointed out by Montgomery [37], the main purpose of Statistical Process Control (SPC) is a fast detection of the occurrence of any assignable causes of process shifts. Accordingly, an optimal design of a control chart is vitally viewed in SPC in order to obtain a fast detection speed of any out-of-control situation. Since the approach proposed by Epprecht, Loureiro, and Chakraborti [18] is easier to be incorporated into the optimal designs of the chart's parameters, it is recommended to be used together with the proposed optimal designs of the VSI EWMA \bar{X} chart with estimated process parameters in this paper.

5. Optimal designs of the VSI EWMA \bar{X} chart with estimated process parameters

This section presents two optimal designs of the VSI EWMA \bar{X} chart with estimated process parameters, i.e. by minimizing the (i) $AATS_1(\delta_{opt})$ and (ii) $EAATS_1(\delta_{min}, \delta_{max})$ for deterministic and unknown shift sizes, respectively. Here, δ_{opt} is the magnitude of the desired mean shift for which a quick detection is needed; while δ_{min} and δ_{max} are the lower and upper bounds of the mean shift, respectively. Two optimization programs, for solving the optimal design models in (i) and (ii), are developed using the ScicosLab (<http://www.scicoslab.org/>) software to compute the optimal parameters (λ, K_1, K_2) of the VSI EWMA \bar{X} chart with estimated process parameters. These programs can be requested from the first author. By taking the parameter estimation into consideration, new combinations of the optimal chart's parameters (λ, K_1, K_2) will be computed accordingly so that the values of $AATS_1$ and $EAATS_1$ are minimized.

5.1 AATS optimization for the VSI EWMA \bar{X} chart with estimated process parameters

The first proposed optimal design is the AATS optimization of the VSI EWMA \bar{X} chart with estimated process parameters for sensitizing the detection of a specific shift in the mean. This optimization model is mathematically written as

$$\underset{\lambda, K_1, K_2}{\text{Minimize}} AATS_1(\delta_{opt}), \quad (29)$$

subject to

$$(i) \quad AATS_0 = \tau \text{ and} \quad (30)$$

$$(ii) \quad AASI_0 = h, \quad (31)$$

where τ is the desired in-control AATS value and h is the desired in-control AASI ($AASI_0$) value. In the rest of this paper, we assume that $AATS_0 = \tau = 370.40$ and $AASI_0 = h = 1$. It is common to adopt $AASI_0 = 1$ time unit as the sampling interval for the FSI-type chart (h_F) is set equal to $h_F = 1$ time unit (Castagliola, Celano and Fichera [7]). This will ensure that both the FSI-type and VSI-type control charts have $AATS_0 = 370.40$ time units.

Using the above optimization model (29) – (31), the steps for obtaining the optimal (λ, K_1, K_2) combination of the VSI EWMA \bar{X} chart with estimated process parameters are illustrated as follows:

Step 1: Specify $m, n, h, h_1, h_2, \delta_{opt}$ and τ .

Step 2: For every $\lambda \in \{0.01, 0.011, 0.012, \dots, 0.999, 1\}$, determine K_1 and K_2 by means of a nonlinear equation solver to satisfy constraint (30), i.e. $AATS_0 = \tau$ and constraint (31), i.e. $AASI_0 = h$. Hence, all the possible (λ, K_1, K_2) combinations that fulfill the two constraints (30) and (31), when $\delta = 0$, can be obtained in this step.

Step 3: For any $\delta_{\text{opt}} \neq 0$ (out-of-control case), identify the optimal (λ, K_1, K_2) combination that yields the smallest AATS_1 value among all the (λ, K_1, K_2) combinations found in Step 2.

For the VSI EWMA \bar{X} chart with known process parameters, the same optimization model in (29) – (31) is employed; however, the ATS and ASI are used instead of the AATS and AASI.

Tables 3 and 4 present the optimal (λ, K_1, K_2) combinations and their corresponding zero-state $(\text{AATS}_1, \text{ASDTS}_1, \text{SDATS}_1)$ values of the VSI EWMA \bar{X} chart with estimated process parameters ($m \in \{25, 50, 100, 1000, 2000\}$), for $n = 5$, and different combinations of δ_{opt} and (h_1, h_2) . The entries for the case of known process parameters ($m = +\infty$) are also tabulated in the last column of Tables 3 and 4. The optimal chart's parameters (λ, K_1, K_2) , which are displayed in the first row of each cell, are obtained through the optimization model (29) – (31); while the zero-state $(\text{AATS}_1, \text{ASDTS}_1, \text{SDATS}_1)$ and $(\text{ATS}_1, \text{SDTS}_1)$ values, which are displayed in the second row of each cell, are computed from the formulae shown in Sections 3.2 and 3.1, respectively. For example, when $(h_1, h_2) = (4.0, 0.1)$ and $m = 100$, the optimal chart's parameters that minimize zero-state AATS_1 for $\delta_{\text{opt}} = 0.4$, are $(\lambda, K_1, K_2) = (0.149, 0.291, 2.866)$. These optimal chart's parameters give zero-state $(\text{AATS}_1, \text{ASDTS}_1, \text{SDATS}_1) = (4.43, 5.32, 1.27)$ (see Table 4). Here, the zero-state $\text{AATS}_1 = 4.43$ is the smallest zero-state AATS_1 for $\delta_{\text{opt}} = 0.4$, among all the zero-state AATS_1 s computed from all the possible (λ, K_1, K_2) combinations that give zero-state $\text{AATS}_0 = 370.40$ and $\text{AASI}_0 = 1$.

The results in Tables 3 and 4 show that for a fixed value of δ_{opt} , the zero-state $(\text{AATS}_1, \text{ASDTS}_1)$ values generally decrease and approach the zero-state $(\text{ATS}_1, \text{SDTS}_1)$ values as m increases. For example, when $(h_1, h_2) = (1.5, 0.1)$ and $\delta_{\text{opt}} = 0.4$, the zero-state $(\text{AATS}_1, \text{ASDTS}_1)$ values are obtained as $(10.08, 16.31)$ for $m = 25$. These values decrease to $(7.76, 5.72)$ for $m = 100$. When $m = 2000$, these zero-state $(\text{AATS}_1, \text{ASDTS}_1)$ values further decrease to $(7.10, 4.80)$, which are quite similar to the zero-state $(\text{ATS}_1, \text{SDTS}_1) = (7.05, 4.44)$ values for $m = +\infty$ (see Table 3). For large δ_{opt} ($\delta_{\text{opt}} \geq 1.5$), the difference between zero-state $(\text{AATS}_1, \text{ASDTS}_1)$ and $(\text{ATS}_1, \text{SDTS}_1)$ values becomes negligible. As expected, the zero-state SDATS_1 value shown in Tables 3 and 4 decreases as m increases. It is obvious from Tables 3 and 4 that a small optimal λ is adopted for a small δ_{opt} and vice versa, for both the cases of known and estimated process parameters.

The zero-state $(\text{AATS}_1, \text{ASDTS}_1, \text{SDATS}_1)$ values obtained in Tables 3 and 4, are generally larger than those in Table 1. Although the performance of the out-of-control situation shown in Table 1 is better than that in Tables 3 and 4, the performance of the in-control situation, i.e.

the zero-state $AATS_0$ in Table 1 is worse than the desired value of the zero-state $AATS_0 = 370.40$ obtained in Tables 3 and 4. For instance, let us consider $(h_1, h_2) = (1.5, 0.5)$, $m = 25$ and $\delta_{opt} = 0.2$, where the zero-state $(AATS_1, ASDTS_1, SDATS_1) = (70.43, 215.32, 148.80)$ and the desired zero-state $AATS_0 = 370.4$ are acquired with the optimal chart's parameters $(\lambda, K_1, K_2) = (0.020, 0.814, 2.505)$ specially designed for the case of estimated process parameters (see Table 3). However, for the same combination of (h_1, h_2, m, δ) , the zero-state $(AATS_1, ASDTS_1, SDATS_1) = (45.53, 108.60, 72.46)$ and $AATS_0 = 190.18$ are obtained by using the optimal chart's parameters $(\lambda, K_1, K_2) = (0.048, 0.614, 2.484)$ associated with the case of known process parameters (see Table 1). It is expected that a small zero-state $AATS_0$ value will give a small zero-state $AATS_1$ value and vice versa. The zero-state $AATS_0$ values in Table 1 are somewhat very small, especially for small m and the cases of $\delta \leq 1.0$ or in other words, small λ . A small $AATS_0$ value will result in a high false alarm rate. On the contrary, by using the optimization model (29) – (31), Tables 3 and 4 give the optimal chart's parameters (λ, K_1, K_2) that have a desirable zero-state $AATS_0 = 370.40$, which solve the problem of a high false alarm rate in Table 1. In the context of SPC, a low false alarm rate is desirable, so that management does not need to waste unnecessary time and resources to identify non-existing assignable causes.

5.2 EAATS optimization for the VSI EWMA \bar{X} chart with estimated process parameters

In practice, the actual shift size is usually unknown and cannot be exactly specified in advance. This is due to the absence of related historical data. Hence, the performance of the VSI EWMA \bar{X} chart with estimated process parameters will be badly affected if a practitioner adopts the optimal chart's parameters for an assumed fixed shift size when a shift with a different size actually occurs. For example, if $m = 100$, $n = 5$, $(h_1, h_2) = (1.7, 0.3)$, the optimal chart's parameters $(\lambda, K_1, K_2) = (0.370, 0.665, 2.979)$ for $\delta_{opt} = 0.8$ are obtained from Table 3. If the actual mean shift size is $\delta = 0.2$ or 0.4 and the selected parameters $(\lambda, K_1, K_2) = (0.370, 0.665, 2.979)$ are used, the zero-state $(AATS_1, ASDTS_1, SDATS_1) = (69.40, 94.11, 45.28)$ or $(9.31, 10.24, 3.83)$, respectively, are obtained. Then, the relative errors for $\delta \in \{0.2, 0.4\}$ are $\{(159.54\%, 213.60\%, 174.42\%), (48.72\%, 109.84\%, 142.41\%)\}$ corresponding to the zero-state $(AATS_1, ASDTS_1, SDATS_1)$ values shown in Table 3. These relative errors increase as the discrepancy between the expected and the real shift δ increases. Note that the relative error for zero-state $AATS_1$ when the actual shift size is $\delta = 0.2$, is computed as $100\% \times |69.40 - 26.74| / 26.74 = 159.54\%$. The relative errors for both the zero-state $ASDTS_1$ and $SDATS_1$ are obtained in the same way.

In order to cope with the random shift-size problem, the second proposed optimal design is the EAATS optimization of the VSI EWMA \bar{X} chart with estimated process parameters to achieve an overall good detection performance for a specified process shift domain. The EAATS is computed as

$$EAATS = E(AATS) = \int_{\delta_{\min}}^{\delta_{\max}} \int_{-\infty}^{\infty} \int_0^{\infty} f_{\delta}(\delta) ATS f_U(u) f_V(v) dv du d\delta, \quad (32)$$

where $f_{\delta}(\delta)$ is the pdf of the process mean shift δ . Note that EAATS quantifies the average statistical performance of the VSI EWMA \bar{X} chart with estimated process parameters based on a preferred continuous range of mean shift and its density function. The difference between zero-state and steady-state EAATS is that the ATS formula in Equation (32) is obtained through Equation (22) or (23) for zero state or steady state, respectively. For the case of known process parameters, EATS is employed. The computation of EATS is as follows:

$$EATS = E(ATs) = \int_{\delta_{\min}}^{\delta_{\max}} f_{\delta}(\delta) ATs d\delta. \quad (33)$$

Similarly, for the zero-state EATS, Equation (7) for ATS is employed in Equation (33); while Equation (11) for ATS is used in Equation (33), for the calculation of steady-state EATS. Since it is often difficult to identify the actual shape of $f_{\delta}(\delta)$, Castagliola, Celano, and Psarakis [30], Celano et al. [31], and Wu, Shamsuzzaman, and Pan [32] adopted the uniform distribution, $U(\delta_{\min}, \delta_{\max})$ to model the unknown shift sizes. Accordingly, we model the unknown shift size in Equations (32) and (33) by means of a uniform distribution with pdf, $f_{\delta}(\delta) = 1 / (\delta_{\max} - \delta_{\min})$.

The proposed optimization model of the VSI EWMA \bar{X} chart with estimated process parameters by minimizing $EAATS_1$ is represented as follows:

$$\text{Minimize}_{\lambda, K_1, K_2} EAATS_1(\delta_{\min}, \delta_{\max}), \quad (34)$$

subject to

$$(i) \quad EAATS_0 = AATS_0 = \tau \text{ and} \quad (35)$$

$$(ii) \quad AASI_0 = h, \quad (36)$$

where τ is the desired in-control EAATS ($EAATS_0$) value and h is the desired in-control AASI value. Similarly, as in Section 5.1, we assume that $EAATS_0 = AATS_0 = \tau = 370.40$ and $AASI_0 = h = 1$. Using the above optimization model (34) – (36), the steps for obtaining the optimal (λ, K_1, K_2) combination of the VSI EWMA \bar{X} chart with estimated process parameters are illustrated as follows:

Step 1: Specify $m, n, h, h_1, h_2, \delta_{\min}, \delta_{\max}$ and τ .

Steps 2 and 3: Similar to Steps 2 and 3 for the optimization model in (29) – (31), but replace constraints (30) and (31) with constraints (35) and (36), respectively. Also, $AATS_1$ is replaced by $EAATS_1$.

For the VSI EWMA \bar{X} chart with known process parameters, a similar optimization model to that in (34) – (36) is employed; however, the EATS and ASI are used instead of the EAATS and AASI.

To facilitate practitioners in a quick implementation of the proposed chart, the optimal chart's parameters of the VSI EWMA \bar{X} chart with estimated process parameters ($m \in \{25, 50, 100, 1000, 2000\}$) by minimizing the zero-state $EAATS_1$, are provided in Tables 5 and 6. The desired shift interval $[\delta_{\min}, \delta_{\max}] = [0.1, 2.0]$ is considered in Tables 5 and 6. The last column in both tables shows the entries associated with the chart with known process parameters ($m = +\infty$). The optimal chart's parameters (λ, K_1, K_2) with their corresponding minimum zero-state $EAATS_1$ value for different combinations of m and (h_1, h_2) are shown in the first and second rows, respectively, for each combination. By using the particular optimal chart's parameters (λ, K_1, K_2) presented in Tables 5 and 6, the zero-state ($AATS_1, ASDTS_1, SDATS_1$) values are also computed for different shift sizes, $\delta \in \{0.2, 0.4, 0.6, 0.8, 1.0, 1.5, 2.0\}$. For illustration, let us consider $m = 100$ and $(h_1, h_2) = (1.5, 0.1)$, where the optimal chart's parameters obtained are $(\lambda, K_1, K_2) = (0.067, 0.917, 2.710)$ (see Table 6). These optimal chart's parameters give zero-state $EAATS_1 = 5.81$. With the same optimal chart's parameters, the zero-state ($AATS_1, ASDTS_1, SDATS_1$) = (1.39, 0.99, 0.14) are obtained for $\delta = 1.0$ (see Table 6).

From Tables 5 and 6, we observe that the difference between the zero-state $EAATS_1$ and $EATS_1$ decreases as m increases for every (h_1, h_2) combination. For example, if $(h_1, h_2) = (1.5, 0.5)$ and $m = 50$, the minimum zero-state $EAATS_1$ obtained using the optimal chart's parameters $(\lambda, K_1, K_2) = (0.065, 0.723, 2.757)$ is 9.17 (see Table 5). This zero-state $EAATS_1$ decreases to 5.54 and 5.46 when m is 1000 and 2000, respectively. From this example, the zero-state $EAATS_1$ decreases and approaches the zero-state $EATS_1 (= 5.38)$ as m increases. A similar trend appears for the zero-state ($AATS_1, ASDTS_1, SDATS_1$) values across Tables 5 and 6. Furthermore, we notice that the global chart's parameters recorded in Tables 5 and 6 give zero-state ($AATS_1, ASDTS_1, SDATS_1$) values that are close to those displayed in Tables 3 and 4. For instance, when $(h_1, h_2) = (1.7, 0.3)$, $m = 1000$, and $\delta = 0.2$, the zero-state ($AATS_1, ASDTS_1, SDATS_1$) = (20.97, 16.34, 2.85) are obtained with the global chart's parameters $(\lambda, K_1, K_2) = (0.064, 0.625, 2.597)$ (see Table 5); while the zero-state ($AATS_1, ASDTS_1, SDATS_1$) = (20.78, 15.83, 2.73) are obtained with the optimal chart's parameters $(\lambda, K_1, K_2) = (0.058,$

0.632, 2.569) specially designed for $\delta_{\text{opt}} = 0.2$ (see Table 3). Accordingly, the chart's parameters presented in Tables 5 and 6 can be considered as a robust alternative to those shown in Tables 3 and 4.

6. A comparison between the zero-state and steady-state performances of the VSI EWMA \bar{X} chart with known and estimated process parameters

In this section, we compare the run-length performances of the VSI EWMA \bar{X} chart with known and estimated process parameters, for zero-state and steady-state cases. Table 7 presents the (AATS, ASDTS, SDATS) values of the VSI EWMA \bar{X} chart with estimated process parameters, for the zero-state and steady-state cases when $(h_1, h_2) \in \{(1.7, 0.3), (1.9, 0.1)\}$. The values of the performance measures shown in the first row of each cell represent the zero-state case; while those (boldfaced entries) shown in the second row of each cell represent the steady-state case. The formulae shown in Sections 3.1 and 3.2 are used to compute the zero-state and steady-state run lengths of the known-parameter and estimated-parameter cases, respectively. Note that the zero-state and steady-state (AATS, ASDTS, SDATS) performances of the VSI EWMA \bar{X} chart with estimated ($m \in \{25, 50, 100, 1000, 2000\}$) process parameters are displayed in columns two to six; while the zero-state and steady-state (ATS, SDTS) performances of the VSI EWMA \bar{X} chart with known ($m = +\infty$) process parameters are listed in the last column.

For a straight-forward and fair comparison, the same control chart's parameters (λ, K_1, K_2) for $(h_1, h_2) = (1.7, 0.3)$ and $(1.9, 0.1)$, where $\delta_{\text{opt}} = 0.8$ (see Tables 3 and 4, respectively), are used to compute the zero-state and steady-state (AATS, ASDTS, SDATS) values, when $\delta \in \{0.0, 0.2, 0.4, 0.6, 0.8, 1.0, 1.5, 2.0\}$. Specifically, when $(h_1, h_2) = (1.7, 0.3)$, $\delta_{\text{opt}} = 0.8$ and $m = 25$, the control chart's parameters $(\lambda, K_1, K_2) = (0.359, 0.694, 2.988)$ are obtained from Table 3. These control chart's parameters $(\lambda, K_1, K_2) = (0.359, 0.694, 2.988)$ are used to compute the zero-state $(\text{AATS}_1, \text{ASDTS}_1, \text{SDATS}_1) \in \{(116.38, 286.00, 184.86), (3.16, 3.82, 1.95)\}$ and steady-state $(\text{AATS}_1, \text{ASDTS}_1, \text{SDATS}_1) \in \{(115.53, 285.81, 184.57), (3.21, 4.02, 2.15)\}$ when $\delta \in \{0.2, 0.6\}$ (see Table 7). A similar approach is applied for the computation of (ATS, SDTS) of the known-process-parameter case.

The results in Table 7 reveal that the difference between the zero-state and steady-state (AATS, ASDTS, SDATS) is not obvious. For small shifts ($\delta < 0.4$), the steady-state (AATS, ASDTS, SDATS) values are generally lower than their corresponding zero-state counterparts. On the contrary, for large shifts ($\delta \geq 0.6$), the steady-state (AATS, ASDTS, SDATS) values

are generally higher than their corresponding zero-state counterparts. However, these differences are very small and negligible. The same results are obtained for the cases with known process parameters. Similar results are also found in the EWMA \bar{X} and VSI EWMA \bar{X} charts with known process parameters proposed by Lucas and Saccucci [37], and Saccucci, Amin, and Lucas [6], respectively. Therefore, from a practical point of view, the difference between the zero-state and steady-state (AATS, ASDTS, SDATS) values is insignificant and either of these (AATS, ASDTS, SDATS) values suffice to represent the performance of the VSI EWMA \bar{X} chart with estimated process parameters. A similar conclusion for the EWMA \bar{X} chart can also be found in Lucas and Saccucci [37]. Since the VSI EWMA \bar{X} chart is an extension of the EWMA \bar{X} chart, it is expected that similar results and conclusions will be obtained.

7. A real-life application

A real dataset collected from a hard-bake process is used to illustrate the implementation of the optimal VSI EWMA \bar{X} chart with estimated process parameters. These data are taken from Montgomery [38]. The hard-bake process is one of the important steps in the photolithography process. Photolithography is a crucial microfabrication process in semiconductor manufacturing. Optical radiation is applied in photolithography to image the mask on a silicon wafer with a light sensitive polymer called a photoresist. A proper control of the flow width of the photoresist in the hard-bake process is vitally viewed. This is because a very small variation in the thickness of photoresist will result in discolouration of the photoresist film. Therefore, the quality characteristic, Y of interest is the flow width measurement (in microns) for this process.

The Phase-I data consist of $m = 25$ samples, each having $n = 5$ wafers. By using the \bar{X} and R charts, Montgomery [38] showed that these Phase-I data are statistically in-control. Then, the estimates $\hat{\mu}_0 = 1.50561$ and $\hat{\sigma}_0 = 0.13943$ are calculated from Equations (14) and (15), respectively. These estimates will be used for Phase-II process monitoring.

In this example, for the Phase-II process monitoring, we decide to implement the VSI EWMA \bar{X} chart with estimated process parameters by considering the sampling intervals (in hours) of $h_1 = 1.7$ and $h_2 = 0.3$, the zero-state $AATS_0 = 370.40$, as well as $\delta_{opt} = 0.8$. The optimal chart's parameters for zero-state $AATS_0 = 370.40$, $(h_1, h_2) = (1.7, 0.3)$, $m = 25$, $n = 5$ and $\delta_{opt} = 0.8$, are $(\lambda, K_1, K_2) = (0.359, 0.694, 2.988)$ (see Table 3). With these optimal chart's

parameters, the control limits and warning limits of the VSI EWMA \bar{X} chart with estimated process parameters are computed by using Equations (3) and (4), respectively, which give

$$UCL/LCL = \pm K_2 \sqrt{\frac{\lambda}{2-\lambda}} = \pm 2.988 \sqrt{\frac{0.359}{2-0.359}} = \pm 1.39757, \quad (37)$$

and

$$UWL/LWL = \pm K_1 \sqrt{\frac{\lambda}{2-\lambda}} = \pm 0.694 \sqrt{\frac{0.359}{2-0.359}} = \pm 0.32460. \quad (38)$$

In Phase-II process monitoring, 20 additional samples, each having $n = 5$ wafers are collected. The summary statistics of these Phase-II data are provided in Table 8. The VSI EWMA \bar{X} chart with estimated process parameters for monitoring the flow width measurements is plotted in Figure 3. From Figure 3, we observe that the first sample ($i = 1$), with the control statistic $Z_1 = -0.03368$ falls in the safe region. Hence, the next sample ($i = 2$) is collected after a long sampling interval, $h_1 = 1.7$ hours. This process continues until the fourth sample, where $Z_4 = -0.40717$. This Z_4 value falls in the warning region; thus, the next sample ($i = 5$) is taken after a short sampling interval, $h_2 = 0.3$ hours. The procedure for deciding the next sampling interval, continues until the control statistic, Z_i falls beyond the control limits (± 1.39757), indicating an out-of-control situation.

From Figure 3, the VSI EWMA \bar{X} chart with estimated process parameters detects the first out-of-control signal at the 15th sample after 16.8 hours. Also, the chart shows an upward trend from the 12th sample (corresponding to the total elapsed time of 14.5 hours) onwards (see Table 8 and Figure 3). These two situations confirm the occurrence of special causes in the process. Hence, an immediate investigation is needed to identify and eliminate the assignable cause(s).

8. Conclusions

In this paper, a Markov chain approach is adopted to derive the theoretical formulae for the performance measures, i.e. AATS, ASDTS, SDATS, AASI, and EAATS, of the VSI EWMA \bar{X} chart with estimated process parameters under both the zero and steady states. Using these theoretical formulae, one can investigate the run-length properties of the VSI EWMA \bar{X} chart with estimated process parameters in detail. Also, the optimization algorithms can easily be developed by using these theoretical formulae. For optimal implementations, the AATS₁ and EAATS₁ values of the proposed chart are minimized, for deterministic and unknown shift sizes, respectively. Tables of optimal chart's parameters (λ , K_1 , K_2) corresponding to predefined (h_1 , h_2) combinations, are provided to facilitate practitioners in quickly implementing the proposed

chart. The SDATS, which considers practitioner-to-practitioner variability, provides more useful information than the AATS. Therefore, in this paper, the SDATS is employed to identify the necessary number of Phase-I samples for the VSI EWMA \bar{X} chart with estimated process parameters.

This paper clearly shows that the Phase-II performance of the VSI EWMA \bar{X} chart is significantly affected by the estimation of process parameters in Phase-I. A large number of Phase-I samples are needed for the VSI EWMA \bar{X} chart with estimated process parameters to achieve a similar performance to the chart with known process parameters. In practice, taking a large number of Phase-I samples during process start-up is impractical. In order to alleviate this problem, the approach proposed by Epprecht, Loureiro, and Chakraborti [18] is recommended to be applied together with the optimal design algorithms proposed in this paper (see Section 5). Consequently, the false alarm rate can be maintained at a desirable level and a quick detection of an out-of-control situation can be attained.

Since the process parameters are rarely known in practice, control charts with estimated process parameters are receiving growing attention in the context of SPC. We believe that the proposed theoretical and optimization methods warrant a further research in developing new adaptive-type EWMA charts with estimated process parameters. Also, the results in this paper are based on the assumptions of a normal underlying process distribution and the independence of the observations. Thus, future investigations can be conducted when these assumptions are violated.

Acknowledgements

This research is supported by the Universiti Sains Malaysia, Fundamental Research Grant Scheme (FRGS), no. 203/PMATHS/6711603. This research is conducted while the third author (Michael B.C. Khoo) is on sabbatical leave at Universiti Tunku Abdul Rahman, Kampar.

References

- [1] Z. L. Chong, M. B. C. Khoo, W. L. Teoh, W. C. Yeong, and S. Y. Teh, "Group Runs Double Sampling np Control Chart for Attributes," *J Test Eval* 45, no. 6 (November 2017): 2267-2282, <https://doi.org/10.1520/JTE20160226>
- [2] J. H. Kang, J. Yu, and S. B. Kim, "Adaptive Nonparametric Control Chart for Time-Varying and Multimodal Processes," *J Process Contr* 37, no. 1 (January 2016): 34-45, <https://doi.org/10.1016/j.jprocont.2015.11.005>
- [3] W. L. Teoh, M. B. C. Khoo, P. Castagliola, W. C. Yeong, and S. Y. Teh, "Run-Sum Control Charts for Monitoring the Coefficient of Variation," *Eur J Oper Res* 257, no. 1 (February 2017): 144-158, <https://doi.org/10.1016/j.ejor.2016.08.067>
- [4] W. L. Teoh, J. Y. Lim, M. B. C. Khoo, Z. L. Chong, and W. C. Yeong, "Optimal Designs of EWMA Charts for Monitoring the Coefficient of Variation Based on Median Run

- Length and Expected Median Run Length,” *J Test Eval* 47, no. 1 (January 2019): 459-479, <https://doi.org/10.1520/JTE20170118>
- [5] W. C. Yeong, S. L. Lim, M. B. C. Khoo, M. H. Chuah, A. X. J. Lim, “The Economic and Economic-Statistical Designs of the Synthetic Coefficient of Variation Chart,” *J Test Eval* 46, no. 3 (May 2018): 1-21, <https://doi.org/10.1520/JTE20160500>
- [6] M. S. Saccucci, R. W. Amin, and J. M. Lucas, “Exponentially Weighted Moving Average Control Schemes with Variable Sampling Intervals,” *Commun Stat Simul Comput* 21, no. 3 (January 1992): 627-657, <https://doi.org/10.1080/03610919208813040>
- [7] P. Castagliola, G. Celano, S. Fichera, “Evaluation of the Statistical Performance of a Variable Sampling Interval R EWMA Control Chart,” *Qual Technol Quant Manag* 3, no. 3 (May 2006): 307-323, <https://doi.org/10.1080/16843703.2006.11673117>
- [8] P. Castagliola, G. Celano, S. Fichera, and F. Giuffrida, “A Variable Sampling Interval S^2 -EWMA Control Chart for Monitoring the Process Variance,” *Int J Technol Manag* 37, no. 1-2 (January 2007): 125-146, <https://doi.org/10.1504/IJTM.2007.011807>
- [9] Y. C. Lin, and C. Y. Chou, “Robustness of the EWMA and the Combined \bar{X} EWMA Control Charts with Variable Sampling Intervals to Non-normality,” *J Appl Stat* 38, no. 3 (January 2011): 553-570, <https://doi.org/10.1080/02664760903521443>
- [10] C. Y. Chou, C. H. Chen, and H. R. Liu, “Economic Design of EWMA Charts with Variable Sampling Intervals,” *Qual Quant* 40, no. 6 (December 2006): 879-896, <https://doi.org/10.1007/s11135-005-8822-8>
- [11] L. Xue, J. Xu, and Y. Liu, “Economic-Statistical Design of Variable Sampling Intervals EWMA Charts under Non-normality,” *Asian J Qual* 11, no. 3 (September 2010): 277-287, <https://doi.org/10.1108/15982681011094023>
- [12] S. F. Yang, “Using a New VSI EWMA Average Loss Control Chart to Monitor Changes in the Difference Between the Process Mean and Target and/or the Process Variability,” *Appl Math Modelling* 37, no. 16-17 (September 2013): 7973-7982, <https://doi.org/10.1016/j.apm.2013.03.023>
- [13] W. C. Yeong, M. B. C. Khoo, L. K. Tham, W. L. Teoh, and M. A. Rahim, “Monitoring the Coefficient of Variation Using a Variable Sampling Interval EWMA Chart,” *J Qual Technol* 49, no. 4 (October 2017): 380-401, <https://doi.org/10.1080/00224065.2017.11918004>
- [14] S. F. Yang, and Y. N. Yu, “Monitoring Cascade Processes Using VSI EWMA Control Charts,” *J Chemom* 23, no. 9-10 (August 2009): 449-462, <https://doi.org/10.1002/cem.1234>
- [15] S. F. Yang, and Y. N. Yu, “Using VSI EWMA Charts to Monitor Dependent Process Steps with Incorrect Adjustment,” *Expert Syst Appl* 36, no. 1 (January 2009): 442-454, <https://doi.org/10.1016/j.eswa.2007.09.036>
- [16] W. A. Jensen, L. A. Jones-Farmer, C. W. Champ, and W. H. Woodall, “Effects of Parameter Estimation on Control Chart Properties: A Literature Review,” *J Qual Technol* 38, no. 4 (October 2006): 349-364, <https://doi.org/10.1080/00224065.2006.11918623>
- [17] S. Psarakis, A. K. Vyniou, and P. Castagliola, “Some Recent Developments on the Effects of Parameter Estimation on Control Charts,” *Qual Reliab Eng Int* 30, no. 8 (December 2014): 1113-1129, <https://doi.org/10.1002/qre.1556>
- [18] E. K. Epprecht, L. D. Loureiro, and S. Chakraborti, “Effect of the Amount of Phase I Data on the Phase II Performance of S^2 and S Control Charts,” *J Qual Technol* 47, no. 2 (April 2015): 139-155, <https://doi.org/10.1080/00224065.2015.11918121>
- [19] L. A. Jones, C. W. Champ, and S. E. Rigdon, “The Performance of Exponentially Weighted Moving Average Charts with Estimated Parameters,” *Technometrics* 43, no. 2 (May 2001): 156-167, <https://doi.org/10.1198/004017001750386279>

- [20] R. D. C. Quinino, L. L. Ho, and A. L. G. Trindade, "Estimation in \bar{X} Control Charts: Effects and Corrections," *Int J Adv Manuf Tech* 72, no. 1-4 (April 2014): 101-106, <https://doi.org/10.1007/s00170-013-5605-6>
- [21] L. A. Jones, "The Statistical Design of EWMA Control Charts with Estimated Parameters," *J Qual Technol* 34, no. 3 (July 2002): 277-288, <https://doi.org/10.1080/00224065.2002.11980158>
- [22] M. Hany, and M. A. Mahmoud, "An Evaluation of the Crosier's CUSUM Control Chart with Estimated Parameters," *Qual Reliab Eng Int* 32, no. 5 (July 2016): 825-835, <https://doi.org/10.1002/qre.1916>
- [23] S. L. Lim, M. B. C. Khoo, W. L. Teoh, and M. Xie, "Optimal Designs of the Variable Sample Size and Sampling Interval \bar{X} Chart When Process Parameters are Estimated," *Int J Prod Econ* 166, no. 8 (August 2015): 20-35, <https://doi.org/10.1016/j.ijpe.2015.04.007>
- [24] N. A. Saleh, M. A. Mahmoud, L. A. Jones-Farmer, I. Zwetsloot, and W. H. Woodall, "Another Look at the EWMA Control Chart with Estimated Parameters," *J Qual Technol* 47, no. 4 (October 2015): 363-382, <https://doi.org/10.1080/00224065.2015.11918140>
- [25] W. L. Teoh, M. B. C. Khoo, P. Castagliola, and S. Chakraborti, "A Median Run Length-Based Double-Sampling \bar{X} Chart with Estimated Parameters for Minimizing the Average Sample Size," *Int J Adv Manuf Tech* 80, no. 1-4 (September 2015): 411-426, <https://doi.org/10.1007/s00170-015-6949-x>
- [26] Y. Zhang, P. Castagliola, Z. Wu, and M. B. C. Khoo, "The Synthetic \bar{X} Chart with Estimated Parameters," *IIE Trans* 43, no. 9 (June 2011): 676-687, <https://doi.org/10.1080/0740817X.2010.549547>
- [27] M. A. Jones, and S. H. Steiner, "Assessing the Effect of Estimation Error on Risk-Adjusted CUSUM Chart Performance," *Int J Qual Health Care* 24, no. 2 (April 2012): 176-181, <https://doi.org/10.1093/intqhc/mzr082>
- [28] A. Faraz, W. H. Woodall, and C. Heuchenne, "Guaranteed Conditional Performance of the S^2 Control Chart with Estimated Parameters," *Int J Prod Research* 53, no. 14 (February 2015): 4405-4413, <https://doi.org/10.1080/00207543.2015.1008112>
- [29] M. Zhang, F. M. Megahed, and W. H. Woodall, "Exponential CUSUM Charts with Estimated Control Limits," *Qual Reliab Eng Int* 30, no. 2 (March 2014): 275-286, <https://doi.org/10.1002/qre.1495>
- [30] P. Castagliola, G. Celano, and S. Psarakis, "Monitoring the Coefficient of Variation Using EWMA Charts," *J Qual Technol* 43, no. 3 (July 2011): 249-265, <https://doi.org/10.1080/00224065.2011.11917861>
- [31] G. Celano, P. Castagliola, S. Fichera, and G. Nenes, "Performance of t Control Charts in Short Runs with Unknown Shift Sizes," *Comput Ind Eng* 64, no. 1 (January 2013): 56-68, <https://doi.org/10.1016/j.cie.2012.10.003>
- [32] Z. Wu, M. Shamsuzzaman, and E. S. Pan, "Optimization Design of Control Charts Based on Taguchi's Loss Function and Random Process Shifts," *Int J Prod Research* 42, no. 2 (January 2004): 379-390, <https://doi.org/10.1081/00207540310001614169>
- [33] M. R. Reynolds, R. W. Amin, J. C. Arnold, and J. A. Nachlas, " \bar{X} Charts with Variable Sampling Intervals," *Technometrics* 30, no. 2 (May 1988): 181-192, <https://doi.org/10.1080/00401706.1988.10488366>
- [34] D. Brook, and D. A. Evans, "An Approach to the Probability Distribution of CUSUM Run Length," *Biometrika* 59, no. 3 (December 1972): 539-549, <https://doi.org/10.1093/biomet/59.3.539>
- [35] J. N. Darroch, and E. Seneta, "On Quasi-stationary Distributions in Absorbing Discrete Time Finite Markov Chains," *J Appl Probab* 2, no. 1 (June 1965): 88-100, <https://doi.org/10.1017/S0021900200031600>

- [36] A. Gandy, and J. T. Kvaløy, “Guaranteed Conditional Performance of Control Charts Via Bootstrap Methods,” *Scand J Stat* 40, no. 4 (December 2013): 647-668, <https://doi.org/10.1002/sjos.12006>
- [37] J. M. Lucas, and M. S. Saccucci, “Exponentially Weighted Moving Average Control Schemes: Properties and Enhancements,” *Technometrics* 32, no. 1 (February 1990): 1-12, <https://doi.org/10.1080/00401706.1990.10484583>
- [38] D. C. Montgomery, *Statistical Quality Control: A Modern Introduction*, 7th ed. (New York: John Wiley & Sons, 2013).

Appendix: Derivation of the transitions probability $\hat{R}_{k,\gamma}$ in Equation (17), for the VSI EWMA \bar{X} chart with estimated process parameters

The transition probability from transient state k to transient state γ is given as

$$\hat{R}_{k,\gamma} = \Pr(Z_i \text{ is in state } \gamma | Z_{i-1} \text{ is in state } k), \quad (\text{A.1})$$

which is equivalent to

$$\hat{R}_{k,\gamma} = \Pr(H_\gamma - d < Z_i < H_\gamma + d | Z_{i-1} = H_k). \quad (\text{A.2})$$

By substituting Z_i in Equation (1) into Equation (A.2) and replacing W_i in Equation (1) with \hat{W}_i , followed by some rearrangements, we obtain

$$\hat{R}_{k,\gamma} = \Pr\left(\frac{H_\gamma - d - (1-\lambda)H_k}{\lambda} < \hat{W}_i < \frac{H_\gamma + d - (1-\lambda)H_k}{\lambda}\right). \quad (\text{A.3})$$

Then, by substituting \hat{W}_i in Equation (16) into Equation (A.3) and with some rearrangements, we get

$$\hat{R}_{k,\gamma} = \Pr\left(\frac{\hat{\sigma}_0}{\sqrt{n}}\left(\frac{H_\gamma - d - (1-\lambda)H_k}{\lambda}\right) + \hat{\mu}_0 < \bar{Y}_i < \frac{\hat{\sigma}_0}{\sqrt{n}}\left(\frac{H_\gamma + d - (1-\lambda)H_k}{\lambda}\right) + \hat{\mu}_0\right). \quad (\text{A.4})$$

Since $\bar{Y}_i \sim N(\mu_0 + \delta\sigma_0, \sigma_0^2/n)$, Equation (A.4) is simplified to

$$\begin{aligned} \hat{R}_{k,\gamma} = & \Phi\left[V\left(\frac{H_\gamma + d - (1-\lambda)H_k}{\lambda}\right) + \frac{U}{\sqrt{m}} - \delta\sqrt{n}\right] - \\ & \Phi\left[V\left(\frac{H_\gamma - d - (1-\lambda)H_k}{\lambda}\right) + \frac{U}{\sqrt{m}} - \delta\sqrt{n}\right], \end{aligned} \quad (\text{A.5})$$

where V and U are defined in Equations (18) and (19), respectively.

Table 1. Zero-state AATs, ASDTs and SDATs of the VSI EWMA \bar{X} chart, together with the chart's parameters (λ, K_1, K_2) corresponding to the case of known process parameters when zero-state $ATS_0 = 370.40$, $ASI_0 = 1$, $n = 5$, and $m \in \{25, 50, 100, 1000, 2000, +\infty\}$.

δ	(λ, K_1, K_2)	$m = 25$	$m = 50$	$m = 100$	$m = 1000$	$m = 2000$	$m = +\infty$
		(AATS ₀ , ASDTS ₀ , SDATS ₀) (AATS ₁ , ASDTS ₁ , SDATS ₁)	(AATS ₀ , ASDTS ₀ , SDATS ₀) (AATS ₁ , ASDTS ₁ , SDATS ₁)	(AATS ₀ , ASDTS ₀ , SDATS ₀) (AATS ₁ , ASDTS ₁ , SDATS ₁)	(AATS ₀ , ASDTS ₀ , SDATS ₀) (AATS ₁ , ASDTS ₁ , SDATS ₁)	(AATS ₀ , ASDTS ₀ , SDATS ₀) (AATS ₁ , ASDTS ₁ , SDATS ₁)	(AATS ₀ , ASDTS ₀ , SDATS ₀) (AATS ₁ , ASDTS ₁ , SDATS ₁)
$(h_1, h_2) = (1.5, 0.5)$							
0.2	(0.048, 0.614, 2.484)	(190.18, 301.48, 170.63) (45.53, 108.60, 72.46)	(224.31, 289.61, 137.11) (31.95, 53.05, 33.87)	(261.53, 298.14, 112.00) (26.34, 26.47, 13.92)	(348.89, 344.70, 37.50) (23.19, 15.68, 2.73)	(359.57, 353.02, 24.12) (23.05, 15.33, 1.89)	(370.40, 362.38) (22.89, 14.98)
0.4	(0.135, 0.660, 2.779)	(239.38, 392.92, 222.23) (8.66, 12.02, 7.59)	(267.50, 347.85, 160.04) (7.68, 6.28, 2.89)	(297.69, 339.38, 119.29) (7.33, 5.18, 1.71)	(359.26, 360.08, 36.68) (7.08, 4.51, 0.48)	(365.40, 364.21, 24.96) (7.07, 4.47, 0.34)	(370.40, 367.69) (7.05, 4.44)
0.6	(0.242, 0.660, 2.897)	(282.29, 473.75, 269.86) (3.53, 3.07, 1.48)	(300.43, 392.00, 179.29) (3.35, 2.50, 0.87)	(322.16, 367.30, 126.53) (3.27, 2.30, 0.57)	(364.52, 367.32, 38.52) (3.22, 2.14, 0.17)	(368.31, 369.01, 26.83) (3.21, 2.13, 0.12)	(370.40, 369.39) (3.21, 2.12)
0.8	(0.346, 0.657, 2.946)	(314.43, 533.49, 305.15) (1.83, 1.52, 0.60)	(323.37, 422.60, 192.98) (1.77, 1.36, 0.39)	(338.13, 385.80, 132.18) (1.75, 1.29, 0.26)	(367.84, 371.63, 40.09) (1.73, 1.23, 0.08)	(370.36, 371.93, 28.13) (1.73, 1.23, 0.06)	(370.40, 369.94) (1.72, 1.23)
1.0	(0.466, 0.668, 2.974)	(343.15, 585.64, 335.71) (1.05, 0.93, 0.32)	(342.43, 447.93, 204.36) (1.03, 0.86, 0.21)	(350.38, 400.20, 136.95) (1.01, 0.83, 0.15)	(369.39, 373.86, 41.31) (1.00, 0.80, 0.05)	(370.97, 373.12, 29.07) (1.00, 0.80, 0.03)	(370.40, 370.31) (1.00, 0.80)
1.5	(0.785, 0.661, 2.999)	(399.28, 680.10, 389.07) (0.27, 0.41, 0.11)	(377.46, 493.06, 223.92) (0.26, 0.39, 0.07)	(371.87, 425.33, 145.36) (0.26, 0.38, 0.05)	(373.02, 378.46, 43.12) (0.25, 0.37, 0.02)	(373.25, 376.21, 30.38) (0.25, 0.37, 0.01)	(370.40, 370.86) (0.25, 0.37)
2.0	(0.949, 0.668, 3.001)	(419.56, 710.12, 404.80) (0.04, 0.16, 0.03)	(389.00, 506.73, 229.10) (0.04, 0.15, 0.02)	(378.26, 432.35, 147.28) (0.04, 0.14, 0.01)	(373.53, 379.14, 43.34) (0.04, 0.14, 0.00)	(373.37, 376.47, 30.53) (0.04, 0.14, 0.00)	(370.40, 370.96) (0.04, 0.14)
$(h_1, h_2) = (1.3, 0.1)$							
0.2	(0.041, 1.030, 2.428)	(182.41, 295.19, 167.79) (41.03, 104.74, 69.99)	(217.02, 285.61, 136.59) (27.80, 50.61, 32.42)	(255.17, 295.58, 112.93) (22.42, 24.49, 12.79)	(346.83, 345.24, 38.61) (19.48, 14.48, 2.40)	(358.36, 354.23, 24.68) (19.35, 14.17, 1.66)	(370.40, 365.10) (19.21, 13.87)
0.4	(0.153, 1.099, 2.809)	(246.35, 412.91, 235.19) (6.84, 12.22, 7.78)	(273.04, 359.30, 166.42) (5.81, 5.84, 2.65)	(302.09, 347.02, 122.56) (5.47, 4.72, 1.49)	(360.68, 363.29, 37.56) (5.22, 4.07, 0.40)	(366.39, 366.92, 25.72) (5.21, 4.04, 0.28)	(370.40, 369.38) (5.19, 4.01)
0.6	(0.274, 1.127, 2.916)	(292.56, 499.18, 286.29) (2.38, 2.71, 1.26)	(307.81, 405.18, 186.71) (2.22, 2.17, 0.69)	(327.46, 375.37, 130.30) (2.15, 1.99, 0.44)	(365.96, 369.87, 39.61) (2.10, 1.87, 0.13)	(369.33, 371.05, 27.68) (2.09, 1.86, 0.09)	(370.40, 370.31) (2.09, 1.85)
0.8	(0.398, 1.139, 2.960)	(327.49, 563.15, 324.00) (1.06, 1.29, 0.45)	(331.96, 436.95, 200.96) (1.01, 1.16, 0.28)	(343.66, 393.89, 136.13) (0.99, 1.11, 0.19)	(368.55, 373.13, 41.18) (0.97, 1.07, 0.06)	(370.63, 372.90, 28.95) (0.97, 1.07, 0.04)	(370.40, 370.42) (0.97, 1.07)
1.0	(0.522, 1.156, 2.981)	(354.94, 611.97, 352.44) (0.50, 0.74, 0.20)	(349.79, 460.33, 211.46) (0.48, 0.70, 0.13)	(354.89, 406.94, 140.56) (0.47, 0.68, 0.09)	(369.96, 374.98, 42.26) (0.46, 0.66, 0.03)	(371.22, 373.82, 29.76) (0.46, 0.66, 0.02)	(370.40, 370.27) (0.46, 0.66)
1.5	(0.781, 1.148, 2.998)	(398.86, 684.70, 393.27) (0.08, 0.20, 0.04)	(376.81, 494.73, 226.26) (0.07, 0.19, 0.02)	(371.17, 425.77, 146.84) (0.07, 0.19, 0.02)	(372.39, 377.98, 43.55) (0.07, 0.18, 0.00)	(372.63, 375.67, 30.68) (0.07, 0.18, 0.00)	(370.40, 370.83) (0.07, 0.18)
2.0	(0.948, 1.159, 3.000)	(420.18, 716.50, 410.07) (0.01, 0.05, 0.01)	(389.06, 509.32, 231.90) (0.01, 0.04, 0.00)	(378.10, 433.40, 148.99) (0.01, 0.04, 0.00)	(373.23, 378.96, 43.82) (0.01, 0.04, 0.00)	(373.06, 376.23, 30.87) (0.01, 0.04, 0.00)	(370.40, 370.93) (0.01, 0.04)
$(h_1, h_2) = (1.9, 0.1)$							
0.2	(0.058, 0.632, 2.547)	(191.20, 320.79, 183.66) (41.16, 114.93, 76.67)	(225.34, 302.49, 144.86) (26.71, 54.66, 34.83)	(262.78, 308.17, 116.85) (20.80, 26.36, 13.69)	(349.46, 351.27, 38.43) (17.53, 15.21, 2.43)	(359.75, 359.10, 24.93) (17.40, 14.88, 1.68)	(370.40, 368.29) (17.25, 14.56)
0.4	(0.151, 0.664, 2.804)	(243.82, 417.26, 239.76) (5.81, 11.44, 7.22)	(270.70, 360.91, 169.21) (4.90, 5.44, 2.29)	(300.24, 347.77, 124.68) (4.61, 4.52, 1.27)	(360.24, 363.90, 38.24) (4.40, 4.01, 0.35)	(366.11, 367.61, 26.17) (4.39, 3.98, 0.24)	(370.40, 369.97) (4.37, 3.96)
0.6	(0.273, 0.660, 2.918)	(292.39, 510.36, 295.70) (1.87, 2.46, 1.03)	(307.32, 409.80, 191.51) (1.73, 2.04, 0.56)	(327.14, 377.84, 133.38) (1.68, 1.91, 0.36)	(366.37, 371.12, 40.52) (1.64, 1.82, 0.11)	(369.83, 372.28, 28.31) (1.64, 1.81, 0.07)	(370.40, 371.25) (1.63, 1.81)
0.8	(0.390, 0.662, 2.960)	(326.85, 574.32, 333.70) (0.79, 1.16, 0.34)	(331.21, 441.25, 205.76) (0.75, 1.07, 0.21)	(343.25, 396.12, 139.17) (0.73, 1.04, 0.14)	(369.12, 374.40, 42.05) (0.72, 1.01, 0.04)	(371.29, 374.17, 29.55) (0.72, 1.01, 0.03)	(370.40, 371.13) (0.72, 1.00)
1.0	(0.500, 0.666, 2.980)	(352.60, 620.92, 361.10) (0.36, 0.65, 0.14)	(347.98, 463.31, 215.78) (0.35, 0.61, 0.09)	(353.86, 408.38, 143.35) (0.34, 0.60, 0.06)	(370.45, 376.07, 43.06) (0.34, 0.59, 0.02)	(371.84, 374.96, 30.31) (0.34, 0.59, 0.01)	(370.40, 371.09) (0.34, 0.59)
1.5	(0.779, 0.662, 2.998)	(400.83, 701.88, 407.00) (0.06, 0.16, 0.03)	(377.22, 500.54, 231.97) (0.06, 0.15, 0.02)	(371.03, 428.10, 149.97) (0.06, 0.15, 0.01)	(371.91, 378.00, 44.35) (0.06, 0.14, 0.00)	(372.13, 375.58, 31.24) (0.06, 0.14, 0.00)	(370.40, 371.17) (0.06, 0.14)
2.0	(0.950, 0.664, 3.001)	(424.28, 737.87, 426.42) (0.01, 0.04, 0.01)	(390.95, 517.18, 238.67) (0.01, 0.03, 0.00)	(379.11, 437.07, 152.67) (0.01, 0.03, 0.00)	(373.60, 379.81, 44.76) (0.01, 0.03, 0.00)	(373.39, 376.94, 31.52) (0.01, 0.03, 0.00)	(370.40, 371.19) (0.01, 0.03)

Table 2. Zero-state AATSSs, ASDTSs, and SDATSs of the VSI EWMA \bar{X} chart with estimated process parameters, and the minimum number of Phase-I samples, m to obtain a zero-state SDATS of not exceeding 10% of the corresponding zero-state ATS value, when zero-state $ATS_0 = 370.40$, $ASI_0 = 1$, and $n = 5$.

δ	$(m, AATS_0, ASDTS_0, SDATS_0)$	$(m, AATS_0, ASDTS_0, SDATS_0)$	$(m, AATS_0, ASDTS_0, SDATS_0)$
	$(m, AATS_1, ASDTS_1, SDATS_1)$	$(m, AATS_1, ASDTS_1, SDATS_1)$	$(m, AATS_1, ASDTS_1, SDATS_1)$
	$(h_1, h_2) = (1.5, 0.5)$	$(h_1, h_2) = (1.7, 0.3)$	$(h_1, h_2) = (1.3, 0.1)$
0.2	(1100, 350.37, 345.71, 35.30) (1400, 23.10, 15.47, 2.28)	(1100, 350.61, 348.66, 36.08) (1500, 20.22, 14.73, 2.02)	(1100, 348.78, 346.70, 36.38) (1600, 19.38, 14.24, 1.87)
0.4	(1000, 359.55, 360.37, 36.72) (480, 7.11, 4.58, 0.70)	(1100, 360.79, 362.61, 35.53) (530, 5.77, 4.18, 0.57)	(1100, 361.68, 363.89, 35.64) (620, 5.24, 4.11, 0.52)
0.6	(1100, 365.64, 368.05, 36.69) (300, 3.23, 2.18, 0.32)	(1200, 366.68, 369.76, 36.02) (350, 2.44, 1.94, 0.24)	(1200, 367.06, 370.23, 36.03) (400, 2.11, 1.89, 0.21)
0.8	(1200, 368.48, 371.51, 36.48) (230, 1.73, 1.25, 0.17)	(1300, 369.12, 372.54, 35.81) (260, 1.23, 1.08, 0.12)	(1300, 369.49, 373.00, 36.02) (350, 0.97, 1.08, 0.10)
1.0	(1300, 370.35, 373.75, 36.18) (210, 1.01, 0.81, 0.10)	(1300, 370.44, 374.34, 36.87) (240, 0.67, 0.66, 0.07)	(1300, 370.53, 374.43, 37.00) (320, 0.46, 0.66, 0.05)
1.5	(1400, 372.57, 376.58, 36.30) (210, 0.25, 0.38, 0.03)	(1400, 372.60, 376.88, 36.89) (200, 0.16, 0.24, 0.02)	(1400, 372.52, 376.66, 36.73) (130, 0.07, 0.19, 0.01)
2.0	(1400, 373.14, 377.30, 36.52) (80, 0.04, 0.14, 0.00)	(1500, 373.21, 377.37, 35.84) (190, 0.02, 0.09, 0.00)	(1400, 373.13, 377.40, 36.96) (40, 0.01, 0.04, 0.00)
	$(h_1, h_2) = (1.5, 0.1)$	$(h_1, h_2) = (1.9, 0.1)$	$(h_1, h_2) = (4.0, 0.1)$
0.2	(1100, 348.67, 347.89, 36.50) (1600, 18.44, 14.25, 1.81)	(1100, 351.58, 352.92, 36.29) (1900, 17.41, 14.90, 1.72)	(1100, 352.22, 355.84, 36.62) (2000, 16.65, 16.30, 1.65)
0.4	(1100, 361.93, 364.71, 36.14) (630, 4.76, 3.99, 0.47)	(1100, 361.08, 364.33, 36.26) (630, 4.41, 4.03, 0.44)	(1100, 361.23, 365.95, 36.52) (690, 4.08, 4.78, 0.40)
0.6	(1200, 367.94, 371.64, 36.89) (450, 1.85, 1.85, 0.18)	(1200, 367.27, 371.23, 36.83) (430, 1.64, 1.83, 0.16)	(1300, 368.15, 373.25, 36.4) (510, 1.44, 2.20, 0.14)
0.8	(1300, 369.78, 373.60, 36.47) (350, 0.83, 1.02, 0.08)	(1300, 369.58, 373.74, 36.72) (360, 0.72, 1.01, 0.07)	(1400, 369.81, 374.82, 35.74) (360, 0.62, 1.20, 0.06)
1.0	(1400, 370.00, 373.85, 35.87) (340, 0.39, 0.61, 0.04)	(1400, 370.91, 375.09, 36.26) (320, 0.34, 0.59, 0.03)	(1400, 370.76, 376.03, 36.64) (310, 0.29, 0.69, 0.03)
1.5	(1500, 373.13, 377.21, 35.95) (90, 0.06, 0.16, 0.01)	(1500, 372.64, 376.98, 36.19) (160, 0.06, 0.14, 0.01)	(1500, 372.83, 378.22, 36.71) (110, 0.05, 0.15, 0.01)
2.0	(1500, 373.69, 377.89, 36.17) (30, 0.01, 0.04, 0.00)	(1500, 373.20, 377.63, 36.42) (30, 0.01, 0.04, 0.00)	(1500, 373.41, 378.87, 36.94) (40, 0.01, 0.03, 0.00)

Table 3. Optimal chart's parameters (λ, K_1, K_2) and their corresponding zero-state $(AATS_1, ASDTS_1, SDATS_1)$ values of the VSI EWMA \bar{X} chart with estimated process parameters when $n = 5$, zero-state $AATS_0 = 370.40$, $AASI_0 = 1$, and $(h_1, h_2) \in \{(1.5, 0.5), (1.7, 0.3), (1.3, 0.1)\}$.

δ_{opt}	$m = 25$	$m = 50$	$m = 100$	$m = 1000$	$m = 2000$	$m = +\infty$
	(λ, K_1, K_2) (AATS ₁ , ASDTS ₁ , SDATS ₁)	(λ, K_1, K_2) (AATS ₁ , ASDTS ₁ , SDATS ₁)	(λ, K_1, K_2) (AATS ₁ , ASDTS ₁ , SDATS ₁)	(λ, K_1, K_2) (AATS ₁ , ASDTS ₁ , SDATS ₁)	(λ, K_1, K_2) (AATS ₁ , ASDTS ₁ , SDATS ₁)	(λ, K_1, K_2) (ATS ₁ , SDTS ₁)
$(h_1, h_2) = (1.5, 0.5)$						
0.2	(0.020, 0.814, 2.505) (70.43, 215.32, 148.80)	(0.039, 0.751, 2.632) (40.55, 81.37, 54.17)	(0.040, 0.696, 2.569) (30.14, 30.42, 16.79)	(0.045, 0.601, 2.489) (23.56, 15.64, 2.74)	(0.058, 0.621, 2.556) (23.44, 16.34, 2.04)	(0.048, 0.614, 2.484) (22.89, 14.98)
0.4	(0.136, 0.757, 2.915) (10.08, 16.31, 10.65)	(0.131, 0.691, 2.887) (8.39, 6.88, 3.28)	(0.151, 0.674, 2.876) (7.76, 5.72, 1.95)	(0.155, 0.634, 2.825) (7.11, 4.72, 0.51)	(0.165, 0.625, 2.832) (7.10, 4.80, 0.37)	(0.135, 0.660, 2.779) (7.05, 4.44)
0.6	(0.169, 0.743, 2.941) (3.92, 2.90, 1.41)	(0.235, 0.684, 2.957) (3.53, 2.60, 0.92)	(0.243, 0.658, 2.944) (3.38, 2.36, 0.60)	(0.242, 0.642, 2.902) (3.23, 2.15, 0.17)	(0.258, 0.653, 2.909) (3.22, 2.19, 0.12)	(0.242, 0.660, 2.897) (3.21, 2.12)
0.8	(0.341, 0.692, 2.990) (1.91, 1.57, 0.63)	(0.324, 0.682, 2.979) (1.84, 1.37, 0.39)	(0.349, 0.674, 2.975) (1.78, 1.31, 0.27)	(0.344, 0.620, 2.954) (1.72, 1.22, 0.08)	(0.339, 0.621, 2.950) (1.72, 1.21, 0.06)	(0.346, 0.657, 2.946) (1.72, 1.23)
1.0	(0.467, 0.696, 2.991) (1.07, 0.95, 0.33)	(0.462, 0.663, 2.997) (1.05, 0.87, 0.22)	(0.470, 0.661, 2.991) (1.03, 0.84, 0.15)	(0.459, 0.676, 2.974) (1.00, 0.80, 0.04)	(0.459, 0.657, 2.972) (1.00, 0.80, 0.03)	(0.466, 0.668, 2.974) (1.00, 0.80)
1.5	(0.781, 0.698, 2.973) (0.26, 0.40, 0.11)	(0.791, 0.657, 2.994) (0.26, 0.39, 0.07)	(0.784, 0.658, 2.998) (0.26, 0.38, 0.05)	(0.784, 0.658, 2.997) (0.25, 0.37, 0.02)	(0.784, 0.658, 2.997) (0.25, 0.37, 0.01)	(0.785, 0.661, 2.999) (0.25, 0.37)
2.0	(0.953, 0.691, 2.962) (0.04, 0.15, 0.02)	(0.953, 0.666, 2.987) (0.04, 0.15, 0.02)	(0.953, 0.661, 2.995) (0.04, 0.14, 0.01)	(0.951, 0.656, 2.998) (0.04, 0.14, 0.00)	(0.951, 0.656, 2.998) (0.04, 0.14, 0.00)	(0.949, 0.668, 3.001) (0.04, 0.14)
$(h_1, h_2) = (1.7, 0.3)$						
0.2	(0.024, 0.832, 2.545) (67.84, 220.84, 151.98)	(0.037, 0.744, 2.613) (37.20, 80.88, 53.95)	(0.044, 0.690, 2.600) (26.74, 30.01, 16.50)	(0.058, 0.632, 2.569) (20.78, 15.83, 2.73)	(0.057, 0.627, 2.552) (20.46, 15.28, 1.85)	(0.049, 0.606, 2.493) (20.03, 14.30)
0.4	(0.111, 0.758, 2.887) (8.36, 14.09, 9.25)	(0.137, 0.716, 2.891) (6.88, 6.24, 2.91)	(0.139, 0.666, 2.864) (6.26, 4.88, 1.58)	(0.142, 0.662, 2.801) (5.78, 4.15, 0.42)	(0.142, 0.663, 2.795) (5.75, 4.11, 0.29)	(0.142, 0.662, 2.791) (5.72, 4.07)
0.6	(0.234, 0.727, 2.966) (2.94, 2.82, 1.33)	(0.244, 0.677, 2.969) (2.70, 2.27, 0.75)	(0.284, 0.661, 2.960) (2.57, 2.15, 0.51)	(0.253, 0.655, 2.910) (2.44, 1.90, 0.14)	(0.251, 0.663, 2.906) (2.43, 1.89, 0.10)	(0.264, 0.659, 2.912) (2.43, 1.91)
0.8	(0.359, 0.694, 2.988) (1.37, 1.33, 0.49)	(0.401, 0.679, 2.994) (1.31, 1.23, 0.33)	(0.370, 0.665, 2.979) (1.27, 1.13, 0.21)	(0.363, 0.648, 2.954) (1.23, 1.07, 0.06)	(0.357, 0.646, 2.950) (1.23, 1.06, 0.04)	(0.362, 0.666, 2.951) (1.22, 1.06)
1.0	(0.472, 0.697, 2.988) (0.73, 0.76, 0.24)	(0.462, 0.680, 2.997) (0.70, 0.70, 0.15)	(0.478, 0.663, 2.992) (0.69, 0.68, 0.11)	(0.477, 0.672, 2.977) (0.67, 0.65, 0.03)	(0.476, 0.667, 2.975) (0.67, 0.65, 0.02)	(0.477, 0.660, 2.976) (0.67, 0.65)
1.5	(0.781, 0.690, 2.971) (0.16, 0.26, 0.07)	(0.801, 0.682, 2.993) (0.16, 0.26, 0.05)	(0.786, 0.672, 2.998) (0.16, 0.25, 0.03)	(0.784, 0.671, 2.997) (0.15, 0.24, 0.01)	(0.783, 0.664, 2.997) (0.15, 0.24, 0.01)	(0.784, 0.661, 2.999) (0.15, 0.24)
2.0	(0.954, 0.695, 2.959) (0.02, 0.09, 0.01)	(0.952, 0.660, 2.987) (0.02, 0.09, 0.01)	(0.950, 0.663, 2.995) (0.02, 0.09, 0.01)	(0.950, 0.668, 2.999) (0.02, 0.09, 0.00)	(0.942, 0.656, 2.998) (0.02, 0.09, 0.00)	(0.948, 0.668, 3.001) (0.02, 0.09)
$(h_1, h_2) = (1.3, 0.1)$						
0.2	(0.031, 1.345, 2.632) (68.45, 224.12, 153.80)	(0.033, 1.236, 2.585) (37.20, 80.39, 53.71)	(0.041, 1.158, 2.579) (27.89, 30.63, 16.95)	(0.040, 1.051, 2.442) (20.12, 14.79, 2.47)	(0.049, 1.067, 2.500) (19.62, 14.86, 1.78)	(0.041, 1.030, 2.428) (19.21, 13.87)
0.4	(0.101, 1.313, 2.875) (8.22, 13.89, 9.11)	(0.118, 1.205, 2.867) (6.54, 5.90, 2.69)	(0.152, 1.168, 2.874) (5.84, 4.99, 1.62)	(0.135, 1.127, 2.787) (5.35, 4.01, 0.39)	(0.135, 1.110, 2.781) (5.32, 3.97, 0.27)	(0.153, 1.099, 2.809) (5.19, 4.01)
0.6	(0.257, 1.232, 2.973) (2.69, 2.93, 1.39)	(0.289, 1.165, 2.974) (2.38, 2.34, 0.78)	(0.265, 1.149, 2.947) (2.26, 2.04, 0.46)	(0.273, 1.129, 2.919) (2.10, 1.87, 0.13)	(0.266, 1.115, 2.913) (2.09, 1.85, 0.09)	(0.274, 1.127, 2.916) (2.09, 1.85)
0.8	(0.378, 1.206, 2.987) (1.15, 1.34, 0.47)	(0.390, 1.168, 2.988) (1.06, 1.19, 0.29)	(0.422, 1.150, 2.986) (1.01, 1.14, 0.20)	(0.397, 1.145, 2.961) (0.97, 1.07, 0.06)	(0.398, 1.148, 2.960) (0.97, 1.07, 0.04)	(0.398, 1.139, 2.960) (0.97, 1.07)
1.0	(0.507, 1.201, 2.986) (0.54, 0.78, 0.21)	(0.514, 1.180, 2.993) (0.50, 0.72, 0.14)	(0.524, 1.152, 2.994) (0.47, 0.68, 0.09)	(0.518, 1.139, 2.981) (0.46, 0.66, 0.03)	(0.518, 1.137, 2.980) (0.46, 0.66, 0.02)	(0.522, 1.156, 2.981) (0.46, 0.66)
1.5	(0.772, 1.157, 2.974) (0.08, 0.20, 0.04)	(0.779, 1.151, 2.993) (0.07, 0.19, 0.02)	(0.785, 1.156, 2.997) (0.07, 0.19, 0.02)	(0.780, 1.156, 2.996) (0.07, 0.18, 0.00)	(0.780, 1.155, 2.996) (0.07, 0.18, 0.00)	(0.781, 1.148, 2.998) (0.07, 0.18)
2.0	(0.951, 1.171, 2.962) (0.01, 0.04, 0.01)	(0.951, 1.161, 2.982) (0.01, 0.04, 0.00)	(0.959, 1.134, 2.994) (0.01, 0.04, 0.00)	(0.948, 1.142, 2.998) (0.01, 0.04, 0.00)	(0.948, 1.142, 2.998) (0.01, 0.04, 0.00)	(0.948, 1.159, 3.000) (0.01, 0.04)

Table 4. Optimal chart's parameters (λ, K_1, K_2) and their corresponding zero-state $(AATS_1, ASDTS_1, SDATS_1)$ values of the VSI EWMA \bar{X} chart with estimated process parameters when $n = 5$, zero-state $AATS_0 = 370.40$, $AASI_0 = 1$, and $(h_1, h_2) \in \{(1.5, 0.1), (1.9, 0.1), (4.0, 0.1)\}$.

δ_{opt}	$m = 25$	$m = 50$	$m = 100$	$m = 1000$	$m = 2000$	$m = +\infty$
	(λ, K_1, K_2) (AATS ₁ , ASDTS ₁ , SDATS ₁)	(λ, K_1, K_2) (AATS ₁ , ASDTS ₁ , SDATS ₁)	(λ, K_1, K_2) (AATS ₁ , ASDTS ₁ , SDATS ₁)	(λ, K_1, K_2) (AATS ₁ , ASDTS ₁ , SDATS ₁)	(λ, K_1, K_2) (AATS ₁ , ASDTS ₁ , SDATS ₁)	(λ, K_1, K_2) (ATS ₁ , SDTS ₁)
$(h_1, h_2) = (1.5, 0.1)$						
0.2	(0.019, 1.083, 2.472) (66.75, 218.04, 150.34)	(0.033, 1.016, 2.578) (35.56, 80.28, 53.60)	(0.041, 0.940, 2.578) (24.75, 29.27, 16.01)	(0.061, 0.862, 2.583) (18.85, 15.69, 2.67)	(0.059, 0.860, 2.562) (18.49, 15.07, 1.80)	(0.043, 0.844, 2.441) (18.28, 13.88)
0.4	(0.117, 1.010, 2.895) (7.37, 14.19, 9.30)	(0.139, 0.950, 2.891) (5.89, 5.94, 2.70)	(0.140, 0.931, 2.862) (5.29, 4.62, 1.41)	(0.160, 0.890, 2.829) (4.77, 4.00, 0.38)	(0.163, 0.884, 2.827) (4.75, 3.99, 0.27)	(0.156, 0.877, 2.815) (4.71, 3.90)
0.6	(0.243, 1.000, 2.966) (2.37, 2.66, 1.19)	(0.313, 0.945, 2.979) (2.11, 2.29, 0.74)	(0.268, 0.929, 2.949) (1.98, 1.96, 0.41)	(0.273, 0.913, 2.915) (1.89, 1.84, 0.12)	(0.272, 0.922, 2.912) (1.88, 1.83, 0.08)	(0.300, 0.892, 2.931) (1.83, 1.83)
0.8	(0.378, 0.963, 2.985) (0.98, 1.25, 0.41)	(0.389, 0.937, 2.988) (0.90, 1.12, 0.25)	(0.408, 0.911, 2.987) (0.85, 1.06, 0.17)	(0.382, 0.904, 2.960) (0.83, 1.01, 0.05)	(0.379, 0.900, 2.958) (0.82, 1.01, 0.03)	(0.395, 0.900, 2.962) (0.82, 1.01)
1.0	(0.501, 0.955, 2.984) (0.45, 0.71, 0.18)	(0.509, 0.943, 2.993) (0.42, 0.66, 0.11)	(0.567, 0.919, 2.998) (0.40, 0.64, 0.08)	(0.511, 0.904, 2.983) (0.39, 0.61, 0.02)	(0.509, 0.894, 2.981) (0.39, 0.60, 0.02)	(0.502, 0.918, 2.980) (0.39, 0.60)
1.5	(0.773, 0.937, 2.974) (0.07, 0.18, 0.03)	(0.779, 0.925, 2.988) (0.06, 0.17, 0.02)	(0.780, 0.898, 2.999) (0.06, 0.16, 0.01)	(0.777, 0.906, 2.998) (0.06, 0.16, 0.00)	(0.777, 0.906, 2.998) (0.06, 0.16, 0.00)	(0.780, 0.906, 3.000) (0.06, 0.16)
2.0	(0.951, 0.924, 2.962) (0.01, 0.04, 0.01)	(0.954, 0.931, 2.981) (0.01, 0.04, 0.00)	(0.952, 0.913, 2.996) (0.01, 0.04, 0.00)	(0.949, 0.901, 3.000) (0.01, 0.04, 0.00)	(0.949, 0.901, 3.000) (0.01, 0.04, 0.00)	(0.947, 0.912, 3.002) (0.01, 0.03)
$(h_1, h_2) = (1.9, 0.1)$						
0.2	(0.024, 0.826, 2.532) (65.22, 223.73, 153.63)	(0.037, 0.744, 2.608) (33.99, 81.25, 54.04)	(0.044, 0.679, 2.598) (23.50, 29.38, 15.86)	(0.059, 0.635, 2.575) (17.80, 15.45, 2.50)	(0.059, 0.626, 2.564) (17.54, 15.02, 1.71)	(0.058, 0.632, 2.547) (17.25, 14.56)
0.4	(0.116, 0.774, 2.886) (6.83, 13.86, 9.02)	(0.134, 0.714, 2.886) (5.36, 5.70, 2.43)	(0.144, 0.687, 2.858) (4.94, 4.71, 1.35)	(0.151, 0.660, 2.813) (4.42, 4.02, 0.35)	(0.151, 0.664, 2.808) (4.40, 3.99, 0.24)	(0.151, 0.664, 2.804) (4.37, 3.96)
0.6	(0.245, 0.719, 2.965) (2.07, 2.58, 1.08)	(0.263, 0.686, 2.963) (1.85, 2.12, 0.59)	(0.263, 0.661, 2.972) (1.76, 2.04, 0.42)	(0.273, 0.648, 2.922) (1.64, 1.82, 0.11)	(0.273, 0.644, 2.919) (1.64, 1.81, 0.07)	(0.273, 0.660, 2.918) (1.63, 1.81)
0.8	(0.374, 0.695, 2.986) (0.83, 1.20, 0.35)	(0.385, 0.662, 2.993) (0.77, 1.08, 0.21)	(0.388, 0.666, 2.983) (0.75, 1.04, 0.14)	(0.391, 0.655, 2.961) (0.72, 1.01, 0.04)	(0.391, 0.653, 2.960) (0.72, 1.01, 0.03)	(0.390, 0.662, 2.960) (0.72, 1.00)
1.0	(0.491, 0.706, 2.985) (0.38, 0.67, 0.15)	(0.497, 0.672, 2.998) (0.35, 0.62, 0.09)	(0.499, 0.671, 2.993) (0.35, 0.60, 0.06)	(0.501, 0.653, 2.980) (0.34, 0.59, 0.02)	(0.500, 0.662, 2.979) (0.34, 0.59, 0.01)	(0.500, 0.666, 2.980) (0.34, 0.59)
1.5	(0.773, 0.697, 2.968) (0.06, 0.16, 0.03)	(0.777, 0.682, 2.993) (0.06, 0.15, 0.02)	(0.781, 0.672, 2.998) (0.06, 0.15, 0.01)	(0.779, 0.672, 2.997) (0.06, 0.14, 0.00)	(0.780, 0.663, 2.997) (0.06, 0.14, 0.00)	(0.779, 0.662, 2.998) (0.06, 0.14)
2.0	(0.951, 0.683, 2.956) (0.01, 0.04, 0.00)	(0.954, 0.671, 2.986) (0.01, 0.03, 0.00)	(0.951, 0.658, 2.995) (0.01, 0.03, 0.00)	(0.948, 0.659, 2.999) (0.01, 0.03, 0.00)	(0.948, 0.659, 2.999) (0.01, 0.03, 0.00)	(0.950, 0.664, 3.001) (0.01, 0.03)
$(h_1, h_2) = (4.0, 0.1)$						
0.2	(0.023, 0.338, 2.527) (63.63, 226.89, 155.14)	(0.034, 0.326, 2.580) (33.26, 81.43, 53.46)	(0.043, 0.301, 2.592) (22.74, 30.20, 15.34)	(0.053, 0.273, 2.550) (16.89, 16.45, 2.28)	(0.052, 0.273, 2.532) (16.66, 16.07, 1.55)	(0.063, 0.267, 2.578) (16.50, 15.99)
0.4	(0.113, 0.331, 2.880) (6.16, 13.79, 8.64)	(0.138, 0.306, 2.893) (4.81, 6.21, 2.29)	(0.149, 0.291, 2.866) (4.43, 5.32, 1.27)	(0.157, 0.293, 2.813) (4.09, 4.78, 0.34)	(0.158, 0.292, 2.809) (4.07, 4.75, 0.24)	(0.157, 0.283, 2.804) (4.04, 4.72)
0.6	(0.243, 0.304, 2.966) (1.77, 2.85, 0.95)	(0.260, 0.302, 2.954) (1.64, 2.51, 0.53)	(0.268, 0.276, 2.964) (1.49, 2.26, 0.32)	(0.268, 0.268, 2.928) (1.42, 2.16, 0.09)	(0.267, 0.277, 2.925) (1.42, 2.16, 0.07)	(0.317, 0.289, 2.945) (1.43, 2.18)
0.8	(0.362, 0.302, 2.977) (0.72, 1.41, 0.30)	(0.372, 0.320, 2.973) (0.68, 1.33, 0.19)	(0.371, 0.282, 2.988) (0.64, 1.23, 0.12)	(0.374, 0.272, 2.966) (0.62, 1.20, 0.04)	(0.374, 0.271, 2.964) (0.61, 1.20, 0.03)	(0.374, 0.279, 2.964) (0.61, 1.20)
1.0	(0.475, 0.316, 2.977) (0.33, 0.78, 0.12)	(0.476, 0.273, 3.005) (0.30, 0.71, 0.08)	(0.480, 0.292, 3.000) (0.30, 0.70, 0.05)	(0.480, 0.286, 2.985) (0.29, 0.68, 0.02)	(0.476, 0.283, 2.983) (0.29, 0.68, 0.01)	(0.479, 0.290, 2.985) (0.29, 0.68)
1.5	(0.777, 0.311, 2.960) (0.06, 0.17, 0.02)	(0.779, 0.290, 3.000) (0.06, 0.16, 0.02)	(0.780, 0.292, 3.005) (0.05, 0.15, 0.01)	(0.780, 0.287, 3.004) (0.05, 0.15, 0.00)	(0.776, 0.293, 3.004) (0.05, 0.15, 0.00)	(0.777, 0.291, 3.006) (0.05, 0.15)
2.0	(0.952, 0.269, 2.971) (0.01, 0.04, 0.01)	(0.954, 0.271, 2.994) (0.01, 0.03, 0.00)	(0.954, 0.289, 3.002) (0.01, 0.03, 0.00)	(0.949, 0.287, 3.006) (0.01, 0.03, 0.00)	(0.949, 0.293, 3.006) (0.01, 0.03, 0.00)	(0.946, 0.291, 3.008) (0.01, 0.03)

Table 5. Optimal VSI EWMA \bar{X} chart's parameters (λ, K_1, K_2) , zero-state EAATS₁s and the zero-state (AATS₁, ASDTS₁, SDATS₁) values corresponding to the specific shift sizes $\delta \in \{0.2, 0.4, 0.6, 0.8, 1.0, 1.5, 2.0\}$, when zero-state EAATS₀ = 370.40, AASI₀ = 1, $n = 5$, $m \in \{25, 50, 100, 1000, 2000, +\infty\}$ and $(h_1, h_2) \in \{(1.5, 0.5), (1.7, 0.3), (1.3, 0.1)\}$.

δ	$m = 25$	$m = 50$	$m = 100$	$m = 1000$	$m = 2000$	$m = +\infty$
	(λ, K_1, K_2)	(λ, K_1, K_2)	(λ, K_1, K_2)	(λ, K_1, K_2)	(λ, K_1, K_2)	(λ, K_1, K_2)
	EAATS ₁	EAATS ₁	EAATS ₁	EAATS ₁	EAATS ₁	EATS ₁
	(AATS ₁ , ASDTS ₁ , SDATS ₁)	(AATS ₁ , ASDTS ₁ , SDATS ₁)	(AATS ₁ , ASDTS ₁ , SDATS ₁)	(AATS ₁ , ASDTS ₁ , SDATS ₁)	(AATS ₁ , ASDTS ₁ , SDATS ₁)	(ATS ₁ , SDTS ₁)
$(h_1, h_2) = (1.5, 0.5)$						
	(0.062, 0.791, 2.795)	(0.065, 0.723, 2.757)	(0.063, 0.683, 2.697)	(0.068, 0.638, 2.613)	(0.068, 0.636, 2.603)	(0.068, 0.629, 2.593)
	12.80	9.17	7.18	5.54	5.46	5.38
0.2	(74.54, 233.45, 158.62)	(42.53, 88.15, 57.63)	(30.78, 35.26, 19.27)	(24.17, 17.90, 3.17)	(23.82, 17.34, 2.17)	(23.46, 16.79)
0.4	(10.59, 12.28, 8.14)	(9.17, 5.75, 2.70)	(8.59, 4.76, 1.59)	(7.74, 4.08, 0.43)	(7.69, 4.04, 0.30)	(7.64, 4.01)
0.6	(5.31, 2.77, 1.38)	(4.86, 2.36, 0.85)	(4.86, 2.17, 0.56)	(4.67, 2.17, 0.16)	(4.21, 1.97, 0.11)	(4.19, 1.96)
0.8	(3.42, 1.58, 0.68)	(3.15, 1.42, 0.44)	(3.04, 1.34, 0.30)	(2.74, 1.25, 0.09)	(2.73, 1.24, 0.06)	(2.71, 1.24)
1.0	(2.42, 1.10, 0.43)	(2.21, 1.00, 0.28)	(2.14, 0.95, 0.19)	(1.92, 0.88, 0.05)	(1.91, 0.88, 0.04)	(1.90, 0.87)
1.5	(1.20, 0.57, 0.19)	(1.10, 0.50, 0.12)	(1.07, 0.47, 0.08)	(0.95, 0.42, 0.02)	(0.95, 0.42, 0.02)	(0.94, 0.42)
2.0	(0.69, 0.30, 0.10)	(0.65, 0.26, 0.06)	(0.63, 0.24, 0.04)	(0.58, 0.20, 0.01)	(0.57, 0.20, 0.01)	(0.57, 0.19)
$(h_1, h_2) = (1.7, 0.3)$						
	(0.065, 0.801, 2.795)	(0.066, 0.717, 2.757)	(0.061, 0.684, 2.688)	(0.064, 0.625, 2.597)	(0.064, 0.643, 2.586)	(0.065, 0.638, 2.581)
	12.00	8.31	6.30	4.71	4.64	4.56
0.2	(72.06, 236.67, 160.92)	(39.21, 88.03, 57.79)	(27.26, 33.37, 18.38)	(20.97, 16.34, 2.85)	(20.67, 15.85, 1.94)	(20.39, 15.45)
0.4	(9.05, 11.97, 7.83)	(7.73, 5.40, 2.35)	(7.28, 4.54, 1.37)	(6.55, 3.94, 0.37)	(6.51, 3.91, 0.26)	(6.44, 3.88)
0.6	(4.39, 2.68, 1.19)	(4.00, 2.32, 0.73)	(3.88, 2.17, 0.49)	(3.51, 2.00, 0.14)	(3.49, 1.99, 0.10)	(3.45, 1.98)
0.8	(2.76, 1.58, 0.59)	(2.51, 1.44, 0.38)	(2.45, 1.38, 0.26)	(2.20, 1.30, 0.07)	(2.19, 1.29, 0.05)	(2.16, 1.28)
1.0	(1.88, 1.13, 0.37)	(1.70, 1.04, 0.24)	(1.66, 1.01, 0.17)	(1.48, 0.94, 0.05)	(1.47, 0.93, 0.03)	(1.45, 0.93)
1.5	(0.81, 0.59, 0.16)	(0.73, 0.51, 0.10)	(0.72, 0.48, 0.06)	(0.64, 0.42, 0.02)	(0.64, 0.42, 0.01)	(0.62, 0.41)
2.0	(0.41, 0.24, 0.06)	(0.39, 0.20, 0.04)	(0.39, 0.19, 0.03)	(0.36, 0.15, 0.01)	(0.36, 0.15, 0.00)	(0.35, 0.15)
$(h_1, h_2) = (1.3, 0.1)$						
	(0.071, 1.302, 2.820)	(0.073, 1.232, 2.779)	(0.066, 1.179, 2.705)	(0.064, 1.071, 2.597)	(0.063, 1.059, 2.582)	(0.066, 1.066, 2.586)
	12.05	8.32	6.26	4.55	4.48	4.40
0.2	(73.39, 237.60, 161.17)	(40.25, 90.48, 59.05)	(27.41, 35.28, 19.38)	(20.16, 16.44, 2.88)	(19.80, 15.83, 1.95)	(19.64, 15.60)
0.4	(8.52, 12.34, 8.08)	(7.14, 5.33, 2.32)	(6.71, 4.37, 1.30)	(6.02, 3.73, 0.34)	(6.01, 3.70, 0.24)	(5.91, 3.68)
0.6	(4.06, 2.49, 1.08)	(3.67, 2.14, 0.65)	(3.60, 2.00, 0.43)	(3.29, 1.84, 0.12)	(3.29, 1.84, 0.09)	(3.22, 1.82)
0.8	(2.60, 1.42, 0.51)	(2.37, 1.29, 0.33)	(2.35, 1.24, 0.22)	(2.15, 1.17, 0.07)	(2.15, 1.17, 0.05)	(2.09, 1.16)
1.0	(1.85, 0.98, 0.32)	(1.68, 0.92, 0.21)	(1.67, 0.90, 0.15)	(1.52, 0.87, 0.04)	(1.52, 0.87, 0.03)	(1.47, 0.87)
1.5	(0.90, 0.68, 0.19)	(0.77, 0.66, 0.13)	(0.77, 0.65, 0.09)	(0.65, 0.63, 0.03)	(0.65, 0.63, 0.02)	(0.62, 0.62)
2.0	(0.35, 0.49, 0.11)	(0.27, 0.41, 0.06)	(0.26, 0.41, 0.04)	(0.21, 0.34, 0.01)	(0.21, 0.34, 0.01)	(0.20, 0.32)

Table 6. Optimal VSI EWMA \bar{X} chart's parameters (λ, K_1, K_2) , zero-state EAATS₁s and the zero-state (AATS₁, ASDTS₁, SDATS₁) values corresponding to the specific shift sizes $\delta \in \{0.2, 0.4, 0.6, 0.8, 1.0, 1.5, 2.0\}$, when zero-state EAATS₀ = 370.40, AASI₀ = 1, $n = 5$, $m \in \{25, 50, 100, 1000, 2000, +\infty\}$ and $(h_1, h_2) \in \{(1.5, 0.1), (1.9, 0.1), (4.0, 0.1)\}$.

δ	$m = 25$	$m = 50$	$m = 100$	$m = 1000$	$m = 2000$	$m = +\infty$
	(λ, K_1, K_2)	(λ, K_1, K_2)	(λ, K_1, K_2)	(λ, K_1, K_2)	(λ, K_1, K_2)	(λ, K_1, K_2)
	EAATS ₁	EAATS ₁	EAATS ₁	EAATS ₁	EAATS ₁	EATS ₁
	(AATS ₁ , ASDTS ₁ , SDATS ₁)	(AATS ₁ , ASDTS ₁ , SDATS ₁)	(AATS ₁ , ASDTS ₁ , SDATS ₁)	(AATS ₁ , ASDTS ₁ , SDATS ₁)	(AATS ₁ , ASDTS ₁ , SDATS ₁)	(ATS ₁ , SDTS ₁)
$(h_1, h_2) = (1.5, 0.1)$						
	(0.067, 1.078, 2.800)	(0.064, 0.990, 2.746)	(0.067, 0.917, 2.710)	(0.062, 0.869, 2.588)	(0.062, 0.862, 2.577)	(0.062, 0.861, 2.566)
	11.67	7.91	5.81	4.21	4.14	4.07
0.2	(71.19, 237.96, 161.73)	(37.37, 87.82, 57.75)	(25.61, 34.27, 18.91)	(18.89, 15.78, 2.69)	(18.61, 15.30, 1.84)	(18.32, 14.85)
0.4	(8.10, 11.93, 7.75)	(6.90, 5.19, 2.12)	(6.14, 4.33, 1.20)	(5.68, 3.80, 0.32)	(5.64, 3.77, 0.22)	(5.61, 3.75)
0.6	(3.88, 2.55, 1.04)	(3.59, 2.23, 0.64)	(3.59, 2.05, 0.40)	(3.24, 2.05, 0.12)	(3.06, 1.93, 0.08)	(3.02, 1.91)
0.8	(2.46, 1.50, 0.50)	(2.30, 1.39, 0.33)	(2.05, 1.31, 0.22)	(1.94, 1.26, 0.06)	(1.93, 1.26, 0.05)	(1.91, 1.26)
1.0	(1.71, 1.08, 0.32)	(1.59, 1.03, 0.22)	(1.39, 0.99, 0.14)	(1.31, 0.97, 0.04)	(1.30, 0.96, 0.03)	(1.29, 0.96)
1.5	(0.71, 0.73, 0.18)	(0.63, 0.69, 0.12)	(0.51, 0.62, 0.07)	(0.46, 0.59, 0.02)	(0.46, 0.58, 0.01)	(0.45, 0.58)
2.0	(0.24, 0.39, 0.07)	(0.20, 0.33, 0.04)	(0.16, 0.26, 0.02)	(0.15, 0.23, 0.01)	(0.15, 0.22, 0.00)	(0.15, 0.22)
$(h_1, h_2) = (1.9, 0.1)$						
	(0.067, 0.785, 2.792)	(0.067, 0.734, 2.756)	(0.059, 0.675, 2.680)	(0.060, 0.623, 2.580)	(0.060, 0.619, 2.569)	(0.060, 0.624, 2.558)
	11.22	7.46	5.42	3.88	3.81	3.74
0.2	(69.50, 239.65, 163.03)	(35.94, 88.16, 57.99)	(23.74, 31.96, 17.50)	(17.83, 15.51, 2.52)	(17.57, 15.08, 1.72)	(17.30, 14.67)
0.4	(7.56, 11.81, 7.54)	(6.30, 5.32, 2.01)	(5.97, 4.60, 1.16)	(5.36, 4.08, 0.31)	(5.32, 4.06, 0.22)	(5.29, 4.03)
0.6	(3.52, 2.73, 1.00)	(3.14, 2.41, 0.61)	(3.08, 2.29, 0.41)	(2.77, 2.15, 0.12)	(2.75, 2.14, 0.08)	(2.73, 2.13)
0.8	(2.12, 1.67, 0.50)	(1.88, 1.55, 0.32)	(1.87, 1.51, 0.22)	(1.65, 1.43, 0.06)	(1.64, 1.42, 0.04)	(1.63, 1.42)
1.0	(1.37, 1.23, 0.32)	(1.19, 1.14, 0.20)	(1.18, 1.12, 0.14)	(1.02, 1.05, 0.04)	(1.02, 1.05, 0.03)	(1.01, 1.05)
1.5	(0.44, 0.64, 0.12)	(0.37, 0.55, 0.07)	(0.37, 0.54, 0.05)	(0.31, 0.47, 0.01)	(0.31, 0.46, 0.01)	(0.30, 0.46)
2.0	(0.15, 0.22, 0.03)	(0.14, 0.17, 0.02)	(0.14, 0.17, 0.01)	(0.13, 0.13, 0.00)	(0.13, 0.13, 0.00)	(0.13, 0.13)
$(h_1, h_2) = (4.0, 0.1)$						
	(0.051, 0.335, 2.737)	(0.052, 0.318, 2.705)	(0.050, 0.301, 2.628)	(0.056, 0.259, 2.566)	(0.056, 0.261, 2.554)	(0.057, 0.270, 2.548)
	10.57	6.93	5.06	3.51	3.45	3.38
0.2	(65.44, 238.78, 162.79)	(32.90, 84.88, 55.81)	(22.83, 31.29, 16.15)	(16.90, 16.53, 2.33)	(16.66, 16.16, 1.59)	(16.43, 15.82)
0.4	(7.44, 12.16, 7.07)	(6.22, 6.75, 1.99)	(5.93, 6.21, 1.23)	(4.99, 5.34, 0.32)	(4.95, 5.31, 0.22)	(4.90, 5.27)
0.6	(3.24, 3.85, 1.09)	(2.85, 3.41, 0.66)	(2.76, 3.30, 0.44)	(2.31, 2.93, 0.12)	(2.30, 2.92, 0.08)	(2.27, 2.89)
0.8	(1.70, 2.33, 0.51)	(1.49, 2.11, 0.31)	(1.45, 2.06, 0.21)	(1.20, 1.82, 0.06)	(1.19, 1.81, 0.04)	(1.17, 1.80)
1.0	(0.94, 1.52, 0.27)	(0.82, 1.36, 0.16)	(0.80, 1.33, 0.11)	(0.66, 1.15, 0.03)	(0.65, 1.15, 0.02)	(0.64, 1.14)
1.5	(0.28, 0.46, 0.05)	(0.26, 0.39, 0.03)	(0.25, 0.38, 0.02)	(0.22, 0.30, 0.01)	(0.22, 0.30, 0.00)	(0.21, 0.30)
2.0	(0.15, 0.10, 0.02)	(0.15, 0.08, 0.01)	(0.14, 0.08, 0.01)	(0.13, 0.06, 0.00)	(0.13, 0.06, 0.00)	(0.12, 0.06)

Table 7. (AATS, ASDTS, SDATS) values of the VSI EWMA \bar{X} chart with estimated process parameters, for zero-state and steady-state (boldfaced entries) cases when $(h_1, h_2) \in \{(1.7, 0.3), (1.9, 0.1)\}$.

δ	$m = 25$	$m = 50$	$m = 100$	$m = 1000$	$m = 2000$	$m = +\infty$
	(AATS, ASDTS, SDATS)	(AATS, ASDTS, SDATS)	(AATS, ASDTS, SDATS)	(AATS, ASDTS, SDATS)	(AATS, ASDTS, SDATS)	(ATS, SDTS)
$(h_1, h_2) = (1.7, 0.3)$						
0.0	(370.40, 654.68, 381.65) (368.27, 654.64, 381.53)	(370.40, 494.22, 231.16) (368.68, 494.19, 231.08)	(370.40, 426.34, 149.88) (367.83, 426.32, 149.82)	(370.40, 375.29, 41.33) (368.66, 375.29, 41.29)	(370.40, 372.57, 28.71) (368.28, 372.57, 28.68)	(370.40, 369.96) (367.92, 369.95)
0.2	(116.38, 286.00, 184.86) (115.53, 285.81, 184.57)	(90.57, 155.70, 89.69) (89.96, 155.71, 89.69)	(69.40, 94.11, 45.28) (68.79, 94.16, 45.37)	(54.96, 56.24, 9.91) (54.37, 56.26, 9.97)	(53.33, 53.66, 6.76) (52.72, 53.68, 6.79)	(53.31, 52.81) (52.71, 52.82)
0.4	(13.36, 30.47, 19.60) (13.25, 30.59, 19.76)	(11.43, 15.75, 8.02) (11.32, 15.85, 8.17)	(9.31, 10.24, 3.83) (9.18, 10.34, 3.96)	(8.17, 7.68, 0.93) (8.03, 7.74, 0.97)	(7.99, 7.42, 0.63) (7.85, 7.48, 0.67)	(8.04, 7.43) (7.90, 7.49)
0.6	(3.16, 3.82, 1.95) (3.21, 4.02, 2.15)	(3.00, 3.07, 1.14) (3.02, 3.23, 1.27)	(2.74, 2.50, 0.64) (2.76, 2.68, 0.75)	(2.59, 2.22, 0.18) (2.60, 2.39, 0.21)	(2.56, 2.19, 0.12) (2.58, 2.35, 0.15)	(2.57, 2.19) (2.58, 2.36)
0.8	(1.37, 1.33, 0.49) (1.47, 1.62, 0.67)	(1.31, 1.23, 0.33) (1.37, 1.49, 0.43)	(1.27, 1.13, 0.21) (1.33, 1.40, 0.29)	(1.23, 1.07, 0.06) (1.29, 1.34, 0.09)	(1.23, 1.06, 0.04) (1.29, 1.34, 0.06)	(1.22, 1.06) (1.29, 1.33)
1.0	(0.75, 0.73, 0.21) (0.85, 1.10, 0.35)	(0.71, 0.68, 0.15) (0.78, 1.03, 0.23)	(0.71, 0.65, 0.10) (0.78, 1.02, 0.16)	(0.69, 0.63, 0.03) (0.76, 1.00, 0.05)	(0.69, 0.63, 0.02) (0.76, 1.00, 0.04)	(0.69, 0.63) (0.76, 0.99)
1.5	(0.25, 0.24, 0.06) (0.29, 0.77, 0.12)	(0.23, 0.23, 0.04) (0.25, 0.76, 0.07)	(0.24, 0.23, 0.03) (0.27, 0.76, 0.06)	(0.24, 0.22, 0.01) (0.26, 0.75, 0.02)	(0.24, 0.22, 0.01) (0.26, 0.75, 0.01)	(0.24, 0.22) (0.26, 0.75)
2.0	(0.09, 0.14, 0.03) (0.11, 0.71, 0.06)	(0.07, 0.13, 0.02) (0.09, 0.70, 0.03)	(0.08, 0.14, 0.02) (0.10, 0.70, 0.03)	(0.08, 0.13, 0.01) (0.10, 0.70, 0.01)	(0.08, 0.14, 0.00) (0.10, 0.70, 0.01)	(0.08, 0.13) (0.10, 0.70)
$(h_1, h_2) = (1.9, 0.1)$						
0.0	(370.40, 662.31, 387.97) (368.16, 662.26, 387.83)	(370.40, 499.72, 236.36) (368.82, 499.69, 236.27)	(370.40, 429.95, 152.88) (369.07, 429.93, 152.81)	(370.40, 375.38, 42.19) (368.15, 375.37, 42.15)	(370.40, 373.87, 29.53) (369.09, 373.87, 29.50)	(370.40, 371.66) (369.22, 371.66)
0.2	(115.46, 289.90, 187.94) (114.63, 289.71, 187.65)	(84.50, 151.75, 88.97) (83.86, 151.75, 88.96)	(68.76, 95.39, 46.52) (68.16, 95.44, 46.60)	(55.46, 57.69, 10.41) (54.89, 57.70, 10.45)	(54.83, 56.08, 7.22) (54.25, 56.09, 7.25)	(53.96, 54.27) (53.39, 54.28)
0.4	(11.80, 30.27, 19.67) (11.71, 30.37, 19.81)	(8.89, 13.40, 6.97) (8.80, 13.52, 7.13)	(7.81, 9.52, 3.65) (7.70, 9.63, 3.77)	(6.92, 7.25, 0.90) (6.81, 7.33, 0.94)	(6.88, 7.15, 0.63) (6.76, 7.22, 0.66)	(6.81, 7.02) (6.69, 7.10)
0.6	(2.25, 3.39, 1.67) (2.33, 3.61, 1.86)	(1.98, 2.49, 0.82) (2.04, 2.72, 0.96)	(1.87, 2.23, 0.50) (1.92, 2.46, 0.60)	(1.78, 2.04, 0.14) (1.82, 2.26, 0.17)	(1.77, 2.03, 0.10) (1.81, 2.26, 0.12)	(1.76, 2.02) (1.80, 2.24)
0.8	(0.83, 1.20, 0.35) (0.96, 1.57, 0.52)	(0.77, 1.08, 0.21) (0.88, 1.45, 0.32)	(0.75, 1.04, 0.14) (0.84, 1.42, 0.22)	(0.72, 1.01, 0.04) (0.81, 1.38, 0.07)	(0.72, 1.01, 0.03) (0.81, 1.38, 0.05)	(0.72, 1.00) (0.81, 1.38)
1.0	(0.40, 0.67, 0.14) (0.52, 1.17, 0.27)	(0.37, 0.62, 0.09) (0.47, 1.13, 0.17)	(0.36, 0.61, 0.06) (0.46, 1.11, 0.12)	(0.35, 0.60, 0.02) (0.44, 1.10, 0.04)	(0.35, 0.59, 0.01) (0.44, 1.10, 0.03)	(0.35, 0.59) (0.44, 1.10)
1.5	(0.09, 0.18, 0.03) (0.14, 0.93, 0.08)	(0.09, 0.17, 0.02) (0.12, 0.92, 0.05)	(0.09, 0.16, 0.01) (0.12, 0.92, 0.03)	(0.08, 0.16, 0.00) (0.11, 0.92, 0.01)	(0.08, 0.16, 0.00) (0.11, 0.92, 0.01)	(0.08, 0.16) (0.11, 0.92)
2.0	(0.03, 0.05, 0.01) (0.04, 0.90, 0.02)	(0.03, 0.05, 0.01) (0.04, 0.90, 0.01)	(0.02, 0.05, 0.01) (0.03, 0.90, 0.01)	(0.02, 0.05, 0.00) (0.03, 0.90, 0.00)	(0.02, 0.05, 0.00) (0.03, 0.90, 0.00)	(0.02, 0.05) (0.03, 0.90)

Note: The boldfaced values denote the steady-state cases.

Table 8. Summary statistics for the Phase-II data of the flow width measurements (in microns) for the hard-bake process.

Sample number, i	\bar{Y}_i	\hat{W}_i	Z_i	Next sampling interval, h_1 / h_2 hours	Total elapsed time (hours)
1	1.49976	-0.09383	-0.03368	1.7	0.0
2	1.51418	0.13744	0.02775	1.7	1.7
3	1.53324	0.44312	0.17687	1.7	3.4
4	1.41520	-1.44998	-0.40717	0.3	5.1
5	1.50968	0.06527	-0.23757	1.7	5.4
6	1.47240	-0.53262	-0.34349	0.3	7.1
7	1.52920	0.37832	-0.08436	1.7	7.4
8	1.53170	0.41842	0.09614	1.7	9.1
9	1.57934	1.18246	0.48613	0.3	10.8
10	1.42790	-1.24630	-0.13581	1.7	11.1
11	1.48238	-0.37256	-0.22081	1.7	12.8
12	1.49098	-0.23464	-0.22577	1.7	14.5
13	1.61278	1.71876	0.47232	0.3	16.2
14	1.65598	2.41159	1.16852	0.3	16.5
15	1.64202	2.18771	1.53441	*	16.8
16	1.67156	2.66146	1.93902		
17	1.62516	1.91731	1.93123		
18	1.69696	3.06882	2.33962		
19	1.63214	2.02925	2.22820		
20	1.77000	4.24022	2.95052		

Note: The boldfaced values denote the out-of-control cases.

List of figure captions

FIG. 1 A graphical view of the VSI EWMA \bar{X} chart's operation.

FIG. 2 Interval between LCL and UCL divided into $(2g + 1)$ subintervals with each having a width of $2d$.

FIG. 3 The VSI EWMA \bar{X} chart with estimated process parameters, for monitoring the Phase-II data of flow width measurements (in microns) for the hard-bake process.

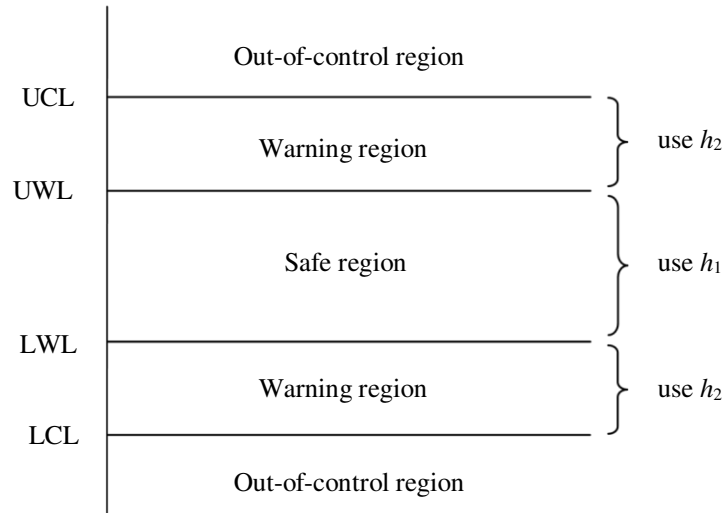


FIG. 1 A graphical view of the VSI EWMA \bar{X} chart's operation.

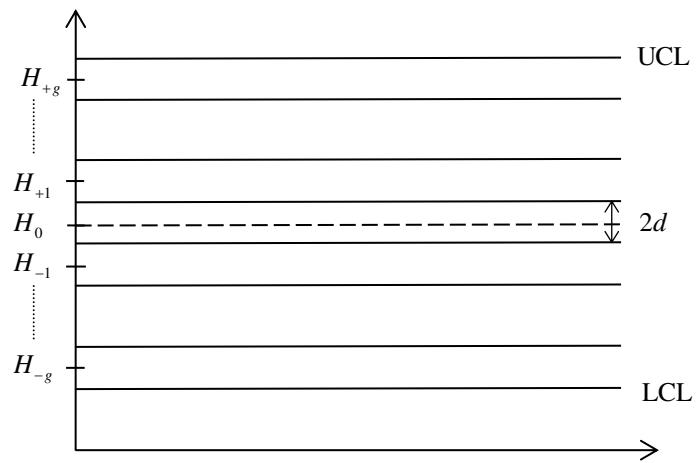


FIG. 2 Interval between LCL and UCL divided into $(2g + 1)$ subintervals with each having a width of $2d$.

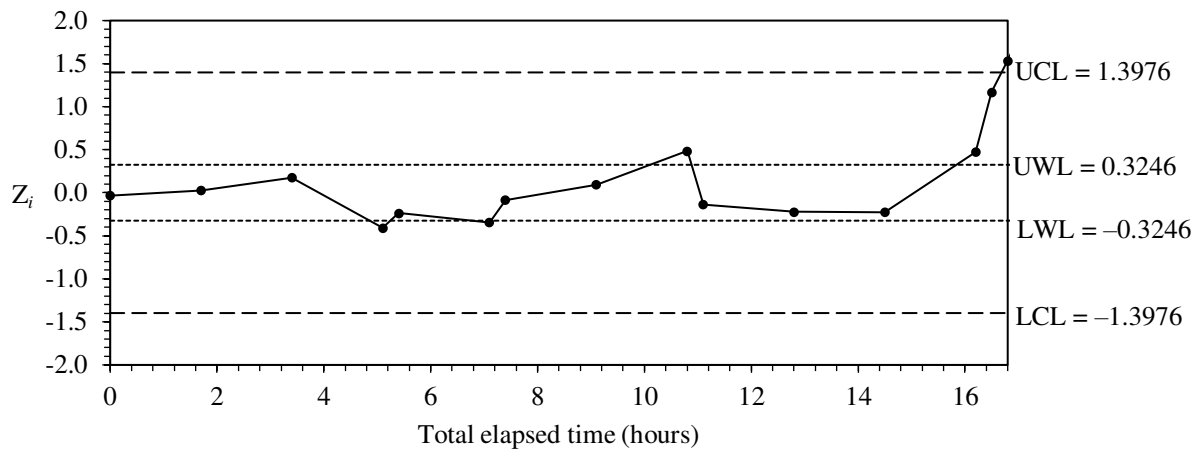


FIG. 3 The VSI EWMA \bar{X} chart with estimated process parameters, for monitoring the Phase-II data of flow width measurements (in microns) for the hard-bake process.